IZMIR KATIP CELEBI UNIVERSITY

GRADUATE SCHOOL OF NATURAL AND APPLIED SCIENCES

EFFECT OF CHANNEL WIDTH ON THE BRIDGE PIER SCOUR

M.Sc. THESIS

Waheedullah MOHAMMAD KHAIL

Department of Civil Engineering

Thesis Advisor: Assoc. Prof. Gökçen BOMBAR

Co-advisor: Prof. Dr António HELENO CARDOSO

August 2020

IZMIR KATIP CELEBI UNIVERSITY

**GRADUATE SCHOOL OF NATURAL AND APPLIED
SCIENCES**

EFFECT OF CHANNEL WIDTH ON THE BRIDGE PIER SCOUR

M.Sc. THESIS

Waheedullah MOHAMMAD KHAIL

(Y180227002)

ORCID NO: 0000-0002-3008-6701

Department of Civil Engineering

Thesis Advisor: Assoc. Prof. Gökçen BOMBAR

Co-advisor: Prof. Dr António HELENO CARDOSO

August 2020

İZMİR KATİP CELEBİ ÜNİVERSİTESİ
FEN BİLİMLERİ ENSTİTÜSÜ

AÇIK KANAL GENİŞLİĞİNİN KÖPRÜ AYAKLARI ETRAFINDA OLUŞAN OYULMALARA ETKİSİ

YÜKSEK LİSANS TEZİ

Waheedullah MOHAMMAD KHAIL

(Y180227002)

ORCID NO: 0000-0002-3008-6701

İnşaat Mühendisliği Bölümü Ana Bilim Dalı

Tez Danışmanı: Doç. Dr. Gökçen BOMBAR

İkinci Danışman: Prof. Dr António HELENO CARDOSO

Ağustos 2020

Waheedullah MOHAMMADKHAIL a M.Sc. student of **IKCU Graduate School Of Natural And Applied Sciences**, successfully defended the thesis entitled **"EFFECT OF CHANNEL WIDTH ON THE BRIDGE PIER SCOUR"**, which he prepared after fulfilling the requirements specified in the associated legislations, before the jury whose signatures are below.

Thesis Advisors:

        Doç. Dr. Gökçen BOMBAR
        İzmir Kâtip Çelebi University

        Prof. Dr. António HELENO CARDOSO
        University of Lisbon, Portugal

Jury Members:

        Doç. Dr. Ebru ERİŞ DUMAN
        Ege University

        Dr. Öğr. Üyesi Erman ÜLKER
        İzmir Kâtip Çelebi University

        Dr. Öğr. Üyesi Oruç ALTINTAŞI
        İzmir Kâtip Çelebi University

Date of Defense   **: 10.08.2020**

To my family

FOREWORD

First and foremost, I would like to thank my advisor, Assoc. Prof. Gökçen BOMBAR and co-advisor Prof. Dr António HELENO CARDOSO for their constant and useful comments, unconditional support and guidance throughout my research work. I feel motivated and encouraged every time I met them.

I would like to thank my dear friends who continuously encourage and support me through this hard time.

Last, but not least, I would like to give my deepest thank to my family, who raised me to these days and didn't hesitate to meet any of my needs.

August 2020   Waheedullah MOHAMMADKHAIL

                                                    (Civil Engineer)

TABLE OF CONTENTS

LIST OF TABLES

LIST OF FIGURES

ABBREVIATIONS

MAE   **:** Mean Absolute Error

PLC   **:** Programmable Logic Controller

RMSE   **:** Root Mean Square Error

B   **:** Channel Width, $[L]$

C   **:** Cohesion, $[M, L^{-1}, T^{-2}]$

b   **:** Pier Diameter, $[L]$

D_*   **:** Dimensionless Grain size

d_{se}   **:** Equilibrium Scour Depth, $[L]$

d_s   **:** Scour Depth, $[L]$

$d_{se,c}$ **:** Calculated Equilibrium Scour Depth, $[L]$

$d_{s,end}$ **:** Scour Depth at End of Experiments, $[L]$

d_{sm}   **:** Maximum Scour Depth, $[L]$

d_{sf}   **:** Final Scour Depth, $[L]$

$\Delta ds/24hr$ **:** Scour Rate per 24 hr, $[L\ T^{-1}]$

d_5   **:** Grain Size Corresponding to 5 % Cumulative Grain Size Distribution curve, $[L]$

d_{10}   **:** Grain Size Corresponding to 10 % Cumulative Grain Size Distribution curve, $[L]$

d_{16}   **:** Grain Size Corresponding to 16 % Cumulative Grain Size Distribution curve, $[L]$

d_{50}   **:** Grain Size Corresponding to 50 % Cumulative Grain Size Distribution curve, $[L]$

d_{60}   **:** Grain Size Corresponding to 60 % Cumulative Grain Size Distribution curve, $[L]$

d_{84}   **:** Grain Size Corresponding to 84 % Cumulative Grain Size Distribution curve, $[L]$

d_{95}	: Grain Size Corresponding to 95 % Cumulative Grain Size Distribution curve, $[L]$
d_g	: Geometric Mean Size
F_d	: Densimetric Particle Froude Number $= V/\sqrt{\Delta\,g\,d_{50}}$
F_{di}	: Densimetric Particle Froude Number for Inception of Sediment Movement in Approach Flow
$F_{d\beta}$	: Densimetric Particle Froude Number of Scour Entrainment
Fr	: Froud Number $= V/\sqrt{gh}$
Fr_{crit}	: Critical Froude Number $= V_c/\sqrt{gh}$
g	: Gravitational Acceleration, $[L\,T^{-2}]$
g'	: Reduced Gravitational Acceleration, $[L\,T^{-2}]$
h	: Approach Flow Depth, $[L]$
H_d	: Dune Height, $[L]$
K_a	: Coefficient for the Effect of River Route
K_b	: Bed Form Shape Factor
K_c	: Coefficient That Shows the Bed Roughness of River
K_D	: Correction Factor of Sediment Coarseness
K_I	: Flow Intensity Factor
K_d	: Grain Shape Factor
K_g	: Pier Group Impact
K_r	: Pier Surface Roughness Factor
K_s	: Pier Shape Factor
K_v	: Impact between Pier Surface and Vertical Angle
K_{yD}	: Depth Dimension Factor
K_α	: Impact Factor of Angle between Approaching Flow and Bridge Axis
K_w	: Correction Factor for Wide Piers
L_p	: Pier Length, $[L]$
n	: Number of Observed or Measured Values
N_s	: Sediment Number

Q **:** Discharge, $[L^3\ T^{-1}]$

P **:** Wetted parameter, $[L]$

R_h **:** Hydraulic Radius, $[L]$

Re **:** Reynolds Number=$4VR_h/v$

$Re_{,pier}$ **:** Pier Reynolds Number=Vb/v

$Re_{,g}$ **:** Grain Size Reynolds Number=Vd_{50}/v

S_o **:** Bed Slop

T **:** Dimensionless Time

T_s **:** Dimensionless Time in Equation, (2.48)

t **:** time, $[T]$

$tanh$ **:** Hyperbolic tan Function

t_{dur} **:** Duration of Experiment Time, $[T]$

t_e **:** equilibrium Time, $[T]$

t_R **:** Reference Time, $[T]$

u_* **:** Shear Velocity, $[L\ T^{-1}]$

u_{*c} **:** Critical Shear Velocity, $[L\ T^{-1}]$

$x_{i,est}$ **:** Estimated or Calculated Value

$x_{i,obt}$ **:** Experimentally Obtained or Measured Value

V **:** Approach Flow Velocity, $[L\ T^{-1}]$

V_c **:** Critical Flow Velocity, $[L\ T^{-1}]$

Z_R **:** Reference Length, $[L]$

α **:** The Angle Between Flow and Pier Axis in the Plan View

Δ **:** Relative Density $=(\rho_s - \rho)/\rho$

v **:** Kinematic Viscosity of the Water, $[L^2\ T^{-1}]$

ρ **:** Density of Water, $[M\ L^{-3}]$

ρ_s **:** Density of Sediment, $[M\ L^{-3}]$

σ_g **:** Gradation Coefficient of Sediment

τ_1 **:** Polynomial Function Coefficient

τ_2 **:** Polynomial Function Coefficient

ℓ_1 **:** Polynomial Function Coefficient

ℓ_2 **:** Polynomial Function Coefficient

h/b   **:** Flow Shallowness

V/V_c **:** Flow Intensity

b/d_{50} **:** Sediment Coarseness

d_s/b **:** Relative Scour Depth

EFFECT OF CHANNEL WIDTH ON THE BRIDGE PIER SCOUR

ABSTRACT

Local scour at the bridge piers and abutments is the main reason for bridges' failure. Thus, scoring around bridge piers is an essential subject in Civil Engineering. Several studies have been conducted to develop and evaluate empirical predictors of local scour time evolution and equilibrium scour depth. Many of these studies were carried out in narrow laboratory flumes, potentially inducing unknown contraction effects in the associated results. The present study intends to investigate the effect of channel width and flow contraction precisely on the temporal evolution and equilibrium scour holes' depth.

The experiments were performed in a 15 m long and 0.90 m high rectangular flume with a horizontal bed made of uniform sand (d_{50}= 1.04 mm; σ_g = 1.16), by imposing three different pier diameters: 74 cm, 120 cm and 177 cm. An electromagnetic flow-meter was used to measure the flow rate and the flow depth was kept constant for all the experiments (h=17 cm). The diameters of tested circular bridge piers were 7 cm, 12 cm and 16 cm and the duration of the experiments was selected to be at least 4 days. The experiments were conducted under the clear-water condition with constant flow intensity (V/Vc= 0.6). Time evolution of the scour was observed and the equilibrium scour depth was determined. The results of the experiments were interpreted in light of the existing literature. After the proper dimensional analysis, it was concluded that dimensionless scour depth, d_{se}/b, is directly proportional with dimensionless flow depth, h/b, whereas changing the dimensionless channel width, b/B, has no appreciable effect on the scour depth as long as the b/B is less than 0.10.

Keywords: bridge pier, channel width, time evolution of scour depth, equilibrium scour depth, clear-water scour

.

AÇIK KANAL GENİŞLİĞİNİN KÖPRÜ AYAKLARI ETRAFINDA OLUŞAN OYULMALARA ETKİSİ

ÖZET

Köprü ayağı etrafında oluşan yerel oyulma köprü yıkılmalarının temel nedenidir. Bu nedenden dolayı köprü ayağı etrafında oluşan oyulma İnşaat Mühendisliği için önemli bir konudur. Yerel oyulma derinliğinin gelişimi ve denge oyulma derinliğini belirlemek ve değerlendirmek için çeşitli çalışmalarla ampirik denklemler geliştirilmiştir. Bu çalışmaların çoğu potansiyel olarak bilinmeyen daralma etkileri ile dar laboratuvar kanallarında gerçekleştirilmiştir. Bu çalışma, kanal genişliği ve akış daralmasının yerel oyulma derinliklerinin zamana bağlı gelişimini, maksimum ve denge üzerindeki etkisini araştırmayı amaçlamaktadır. Deneyler, 15 m uzunluğunda ve 0.90 m yüksekliğinde dikdörtgen biçimli bir kanalda, 74 cm, 120 cm ve 177 cm olmak üzere üç farklı genişlik uygulanarak uniform yatak malzemesinden ($d_{50} = 1.04$ mm, $\sigma_g = 1.16$) oluşan düz bir yatakla gerçekleştirildi. Akım hızını ölçmek için bir elektromanyetik debimetre kullanıldı ve akım derinliği tüm deney için sabit tutuldu ($h = 17$ cm). Test edilen dairesel köprü ayaklarının çapı 7 cm, 12 cm ve 16 cm ve deneylerin süresi en az 4 gün olarak seçildi. Deneyler, sabit akım şiddeti ($V/Vc = 0.6$) olan temiz su koşulu altında gerçekleştirilmiştir. Oyulmanın zamanla gelişimi gözlenir ve denge oyulma derinliği belirlenir. Deneylerin sonuçları mevcut literatür ışığında yorumlanmaktadır. Boyutsal analizden sonra, boyutsuz akış derinliği, h/b'nin boyutsuz oyulma derinliği d_{se}/b ile doğru orantılı olduğu, boyutsuz kanal genişliğindeki b/B değişimin ise b/B değerinin 0,10'dan küçük olduğunda etkili olmadığı gözlenmiştir. .

Anahtar Kelimeler: köprü ayağı, kanal genişliği, zamana bağlı oyulma derinliği, denge oyulma derinliği, temiz su oyulması

1. INTRODUCTION

Local scouring at bridge piers and abutments can induce significant engineering problems. It occurs due to the erosive power of the flow structures acting on the riverbed material in the vicinity of those bridge foundations. Local scour around the bridge foundations is one of the foremost common reasons of bridges' failure. In particular, the existence of bridge piers as on obstruction in the flow modifies the velocity field, increases the local sediment entrainment capacity and can trigger scouring. The combined effects of the 3D velocity field, types of bed material, pier's characteristics and time render scouring a very complex phenomenon.

According to Wardhana and Hadipiriono (2003) scouring is the most important cause of bridges' failure in the United States of America. They stated that 52.88% of bridges collapsed due to scour, whereas earthquakes cause 3.38% of bridge failure [1].

In Turkey, there have been some bridges damages and collapse due to scouring associated with extreme hydraulic events. One recent example was Yayakent Bridge in İzmir which collapsed due to the action of an extreme flood in January 2016 (see Figure 1.1)

Figure 1.1 Yayakent Bridge view after flood in January 2016 [2].

Another example was Çaycuma Bridge over Filyos River that collapsed in 2012, resulting in 15 deaths (see Figure 1.2). According to a report published by the Turkish Association for Bridge and Structural Engineering, the failure happened due to undetermined hydraulic causes [3].

Figure 1.2 Çaycuma Bridge after the flood in 2012 [5].

Devrek Bridge also collapsed due to scouring in 1998 [4], Figure 1.3.

Figure 1.3 Failure due to scour at Devrek Bridge [4].

In addition to the human toll of death, bridges' failure costs millions of dollars each year for renewal and reinstatement. It can also induce the cut of necessary transportation facilities [6]. The USA Federal Highways Administration claimed in 1978 that the failure of bridges and highways resulting from flood events between 1964 and 1972 cost $100 million per event. The same occurs in other countries, as mentioned by [7].

Over the past decades, many researchers have studied the effect of relevant variables and parameters on scouring, including pier diameter or width, flow intensity or bed material characteristics, among others. Most of the research produced until now focused on calculating of the equilibrium scour depth or the time development of the scour depth. Until now, the number of studies on the prediction of the bridge local scour depth attending to the flow contraction is rather reduced. It is believed that further work is needed on this topic.

The aim of the present study is, thus, to investigate the effect of channel width on scouring. In order to deal with that, five experiments were carried out in a 15 m long rectangular channel with two different widths (1.77 m and 0.74 m) and for three different circular piers whose diameters were 7 cm, 12 cm and 16 cm. Three experiments conducted by Kılınc (2019) with the same circular piers in a 1.20 m wide channel were also considered [8]. In all the experiments the discharge, water depth and the bed material characteristics were kept practically constant. The minimum duration of the experiments was 4 days and the maximum was 17 days.

This thesis is organized in 5 chapters.

Chapter 1 is a brief introduction of the thesis.

In Chapter 2, the literature review is offered to cover the current state of the art on local scour around piers; characteristic variables are listed and the effects of independent parameters on the scour mechanism and on the equilibrium scour depth concept are explained. Empirical equations for both equilibrium scour depth and time evolution of the scour are also defined in this chapter.

In Chapter 3 the experimental set-up and procedure are presented and brief information is given on the instrumentation.

Chapter 4 presents the experimental results on the temporal evolution of maximum local scour depth and the equilibrium scour depths obtained with various criteria are compared with empirical equations which exist in the literature. The effect of channel width on the equilibrium scour depth is discussed.

The conclusion is given in Chapter 5

2. LITERATURE REVIEW

2.1 Scour Definition

Scouring is the process of removal of bed grains from the channel bed around the bridge pier. The scour hole is the void left behind when the sediment grains are washed away from the stream bed.

2.2 Type of Scour

According to [9], there are three types of scouring (general scour, contraction scour and local scour), which can be added together. Other authors, e.g. Cheremisinoff et al. (1987), consider only two types of scouring, namely general and localized scour [10]. In this case, contraction scour is considered as part of the localized scour. Other subdivisions of scour are illustrated in Figure 2.1.
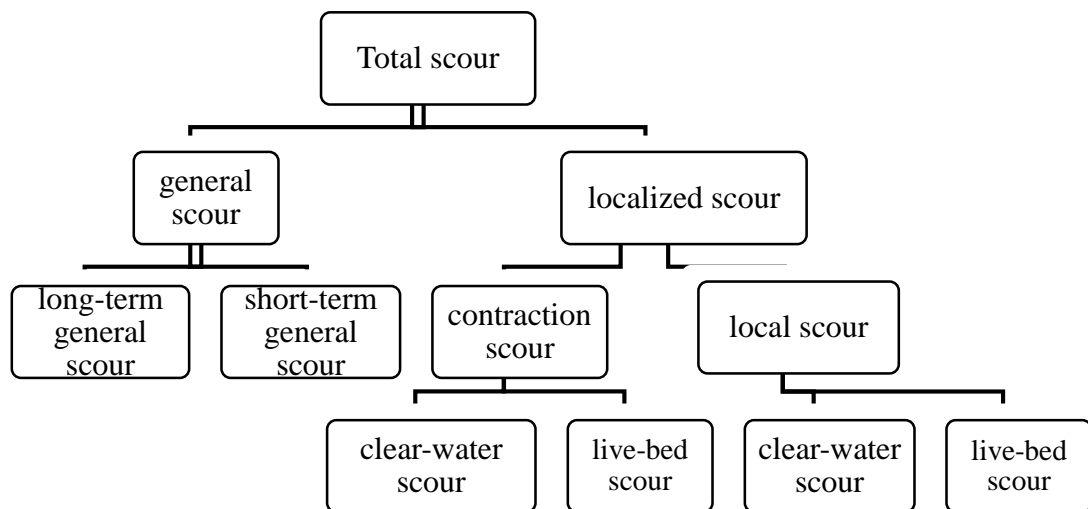
Figure 2.1 An organogram for the various type of scouring [10].

General scour is the scour that influences all or most of the channel bed, taking place mostly during flood events. The principal reasons of general scour are hydro-meteorological, geomorphological and man-made [4]. Scouring can be either short or long-term and it can be observed on riverbeds and banks.

Localized scour differs from general scour. It is directly attributable to the existence of obstacles in the flow, including bridge piers and abutments, and it is circumscribed to the vicinity of these obstacles. According to the logics of Figure 2.1, localized scour is further divided into contraction scour and local scour.

In contraction scour an obstacle decreases the area of the river cross-section which results in the increase of velocity and shear stress, hence, the erosion capacity of the flow [4]. Obstructions on the riverbed accelerate the flow around them producing vortices which trigger bed erosion of the riverbed around their base.

In the case of bridge piers, those vortices include the horseshoe vortex, the surface roller and wake vortices, as seen in Figure 2.2.
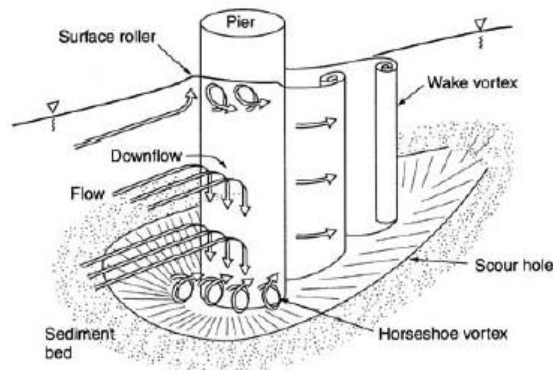
Figure 2.2 Vortex formation in the scour hole [22].

2.3 Dimensional Analysis and Effect of Independent Parameters on Local Scour

Dimensional analysis is an essential tool in formulating local scouring since local scour can be understood better if suitable dimensionless parameters describing the event are defined. Many variables affect scouring, as given below.

Parameter characterizing the fluid

- ρ: density of the water $[M\ L^{-3}]$
- v: kinematic viscosity of the water $[L^2\ T^{-1}]$

Parameter characterizing the flow

- g: gravitational acceleration $[L\ T^{-2}]$
- h: approach flow depth $[L]$

5

- V: approach flow velocity $[\,L\,T^{-1}\,]$
- V_c: critical velocity for the inception of sediment motion $[\,L\,T^{-1}\,]$

Parameter characterizing the channel

- S_o: channel bed slop $[\,-\,]$
- B: channel width $[\,L\,]$
- α: angle between flow and pier axis in the plan view $[\,-\,]$
- K_a: coefficient that shows the effect of river route $[\,-\,]$
- K_b: bed form shape factor $[\,L\,]$
- K_c: coefficient that shows the bed roughness of river $[\,L\,]$

Parameter characterizing the bed material

- ρ_s: density of the sediment $[\,M\,L^{-3}\,]$
- d_{50}: median grain diameter $[\,L\,]$
- σ_g: gradation coefficient of sediment $[\,-\,]$
- C: cohesion $[\,M\,L^{-1}\,T^{-2}\,]$
- K_d: grain shape factor $[\,-\,]$

Parameters characterizing the pier

- b: pier diameter $[\,L\,]$
- K_s: correction factor for pier shape $[\,-\,]$
- K_g: group effect of pier $[\,-\,]$
- K_r: roughness of pier surface $[\,-\,]$
- K_v: impact between the pier and vertical angle $[\,-\,]$

Time

- t: time $[\,T\,]$

The variables, which affect the local scour mechanism, are summarized in the below function.

$$f\begin{pmatrix} d_s, \rho, v, g, h, V, V_c, S_o, B, \alpha, , K_a, K_b, K_c, \\ \rho_s, d_{50}, \sigma_g, C, K_d, b, K_s, K_g, K_r, K_v, t \end{pmatrix} = 0 \qquad (2.1)$$

where d_s is the scour depth. By using the Buckingham Π theorem and selecting ρ, V and b as repeating parameters, the following dimensionless parameter is obtained.

$$\frac{d_s}{b} = f_1 \left(\begin{matrix} \dfrac{V}{\sqrt{gb}}, \dfrac{Vb}{\nu}, \dfrac{h}{b}, \dfrac{V_c}{V}, \dfrac{\rho_s - \rho}{\rho}, \dfrac{Vt}{b}, \dfrac{K_c}{b}, \sigma_g, \dfrac{C}{\rho V^2}, \\[2mm] \dfrac{d_{50}}{b}, \dfrac{K_b}{b}, \dfrac{b}{B}, S_0, \alpha, , K_a, K_d, K_s, K_g, K_r, K_v \end{matrix} \right) \tag{2.2a}$$

After rearranging

$$\frac{d_s}{b} = f_2 \left(\begin{matrix} \dfrac{V}{\sqrt{gh}}, \dfrac{Vd_{50}}{\nu}, \dfrac{h}{b}, \dfrac{V_c}{V}, \dfrac{\rho_s - \rho}{\rho}, \dfrac{Vt}{b}, \dfrac{K_c}{b}, \sigma_g, \dfrac{C}{\rho V^2}, \\[2mm] \dfrac{d_{50}}{b}, \dfrac{K_b}{b}, \dfrac{b}{B}, S_0, \alpha, K_\alpha, K_a, K_d, K_s, K_g, K_r, K_v \end{matrix} \right) \tag{2.2b}$$

In this equation, $V/\sqrt{gh}$ is Froude number (Fr), Vd_{50}/ν, is the particle Reynolds number (Re_g), and $\rho_s - \rho/\rho$ is the submerged relative density, Δ.

Under the specific conditions in this research, the general declaration can be simplified by the following assumption.

- Bed material properties don't change; thus, grain density (ρ_s), grain size (d_{50}), the standard deviation (σ_g), relative density (Δ) and the grain shape factor (K_d) are constant.
- Bed roughness is constant (K_c).
- Bed material is non cohesive ($C=0$), so that $C/\rho V^2$ is dropped.
- Experiments were performed under clear-water conditions and no bed-form was observed (K_b).
- In this study, bed slope is constant.
- Pier surface roughness is constant (K_r). The pier tested is a cylinder (K_s).
- Channel is straight ($K_a=1$).
- Single pier is used, therefore no group effect (K_g).
- Pier is aligned vertically (K_v)

After simplifying the equation (2.2) the equation below is obtained.

$$\frac{d_s}{b} = f_3 \left(Fr, Re_g, \frac{h}{b}, \frac{b}{d_{50}}, \frac{b}{B}, \frac{V_c}{V}, \frac{Vt}{b} \right) \qquad (2.3)$$

The effect of Reynolds number cancels for the fully turbulent flow since viscosity is no longer a characteristic variable of the process. The flow intensity is used rather than the Froude number. For constant V/V_c;

$$\frac{d_s}{b} = f_4 \left(\frac{h}{b}, \frac{b}{d_{50}}, \frac{b}{B}, \frac{Vt}{b} \right) \qquad (2.4)$$

In order to calculate the equilibrium scour depth, d_{se}, the time effect should be ignored as well, and the equation becomes as follows:

$$\frac{d_{se}}{b} = f_5 \left(\frac{h}{b}, \frac{b}{d_{50}}, \frac{b}{B} \right) \qquad (2.5a)$$

After rearranging

$$\frac{d_{se}}{b} = f_6 \left(\frac{h}{b}, \frac{h}{d_{50}}, \frac{b}{B} \right) \qquad (2.5b)$$

The flow depth and the sediment diameter are kept constant, i.e., h/d_{50} is constant. Consequently,

$$\frac{d_{se}}{b} = f_7 \left(\frac{h}{b}, \frac{b}{B} \right) \qquad (2.5c)$$

2.4 Effects of Specific Parameters on Scour Mechanism

2.4.1 Effect of pier size

The equilibrium local scour depth depends on the diameter of the pier [11]. As it can be simply understood from the scour depth predicators (see section 2.5), pier diameter, b, is indeed one of the most important scour variables. Breusers and Raudkivi (1991) even concluded that the pier size affects the time required for the scour hole to approach equilibrium: the bigger the pier diameter the longer the scouring process [12].

2.4.2 Effect of pier shape

The pier shape has an essential effect on the scour depth and process. A schematic illustration of some pier shapes is included in Figure 2.3. The bluntness tends to increase the scour depth for rectangular piers when compared with circular piers [4].
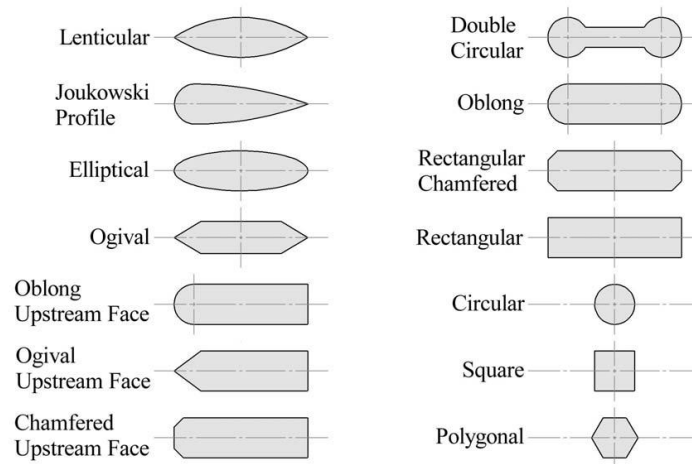
Figure 2.3 Schematic illustration of some pier shapes [14].

Breusers et al. (1977) summarized a few approaches from various authors and claimed that, for a circular or round nosed pier, a scour depth reduction of 25% can be obtained when compared with blunt faced piers [15]. Neill (1978) and Müller and Wagner (2005) concluded that the pier shape does not influence the scour depth in the field as much as in the laboratory [17-18].

The shape factor, K_s, for the Colorado State University (CSU) equation (see section 2.5.6) is given in Table 2.1.

Table 2.1 Correction factor for pier nose shape K_s [16].

SHAPE OF PIER NOSE	K_s
Squares nose	1.1
Round nose	1.0
Circular nose	1.0
Group of cylinders	1.0
Sharp nose	0.9

Fael et al. (2016) studied the effect of pier shape and alignment on the equilibrium scour depth around comparatively short single piers with four different pier shapes. They revealed that the pier shape factor, K_s, is 1.0 for rectangular round-nosed and oblong cross-section piers and 1.2 for rectangular square-nosed and pile-group cross-section piers [19].

2.4.3 Effect of angle of attack

The effect of angle attack has seldom been studied during the past few decades. At single circular piers, the effect of the angle of attack on the scour process is non-existent. Figure 2.4 illustrates the factors, K_α, proposed by [20]. These factors are also described by the following equation established by [20]

$$K_\alpha = \left(cos\alpha + \frac{L}{b}sin\alpha\right)^{0.65} \quad for \quad \alpha > 5^0 \quad 2 < \frac{L}{b} < 16 \quad (2.6)$$

For smaller L/b ratios Fael et al. (2016) suggested the following equations [19]

$$K_\alpha = 1 + \frac{4\alpha}{1000} \qquad for \quad \frac{L}{b} = \frac{4}{3} \qquad (2.7a)$$

$$K_\alpha = 1 + \frac{8\alpha}{1000} \qquad for \quad \frac{L}{b} = 2 \qquad (2.7b)$$
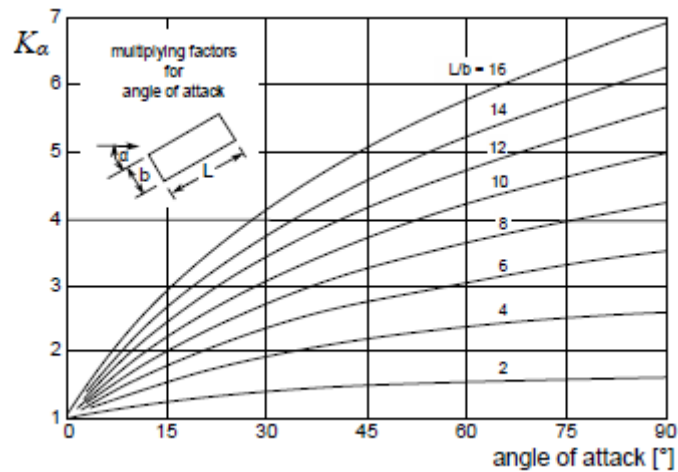
Figure 2.4 Design factor for pier not aligned with the flow according to [20].

2.4.4 Effect of the flow depth

The flow depth, h, has a significant effect on the scour depth (Figure 2.5). For the shallow flows ($h/d < \approx 0.2$) or wide piers ($d/h > \approx 5$), the effect of the surface roller (see Figure 2.2) is important and partly damps the horseshoe vortex in the front of the pier. This effect decreases as the relative flow depth, h/d, increases, leading to the increase of the non-dimensional scour depth with h/b as soon as $h/b < 2 - 2.5$ [21]. If the ratio h/b is larger than $2 - 2.5$, there is no appreciable effect of the flow depth [23]. This upper limit of h/b has been disputed. For instance, Breusers et al. (1977) concluded, after an intense literature and experimental study, that the effect of flow depth can only be ignored for $h/b > 3$ [15]. On the contrary [22] indicate, according to Table 2.2 and Figure 2.5 regarding the classification of piers, that the effect of flow depth is negligible for $h/d > 1/0.7 \approx 1.4$.
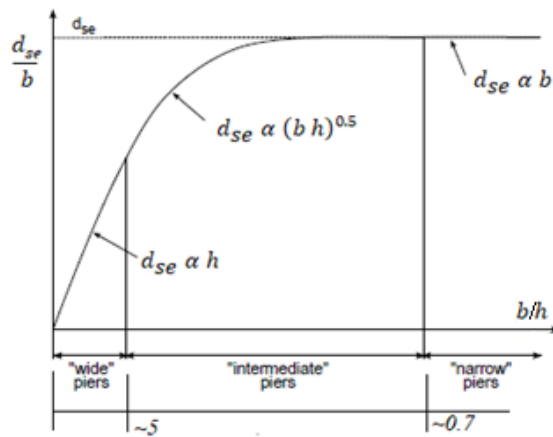
Figure 2.5 Local scour depth variation due to flow shallowness [22].

Table 2.2 Classification of local scour developments at the bridge pier foundations [22].

CLASSIFICATION	RATIO	DEPENDENCY
Narrow	$b/h < 0.7$	$d_{se} \, \alpha \, b$
Intermediate width	$0.7 < b/h < 5$	$d_{se} \, \alpha \, (b \, h)^{0.5}$
Wide	$b/h > 5$	$d_{se} \, \alpha \, h$

Breusers and Raudkivi (1991) found that the finer the sediment relative to pier size, the smaller the effect of flow depth [12].

11

2.4.5 Effect of flow intensity

The ratio of mean flow velocity to critical velocity is called flow intensity (V/V_c). Local scouring can develop in two different conditions, depending on the value of V/V_c: live-bed for $V/V_c > 1.0$ and clear-water for $V/V_c < 1.0$. From the laboratory data of Chabert and Engeldinger, 1956, Shen et al. 1966, Maza Alvarez, 1968, Ettema, 1980; Raudkivi and Ettema, 1983 (among others) the variation of equilibrium scour depth with the flow intensity and the gradation coefficient is as shown in Figure 2.6 [11-25-26-27-28].
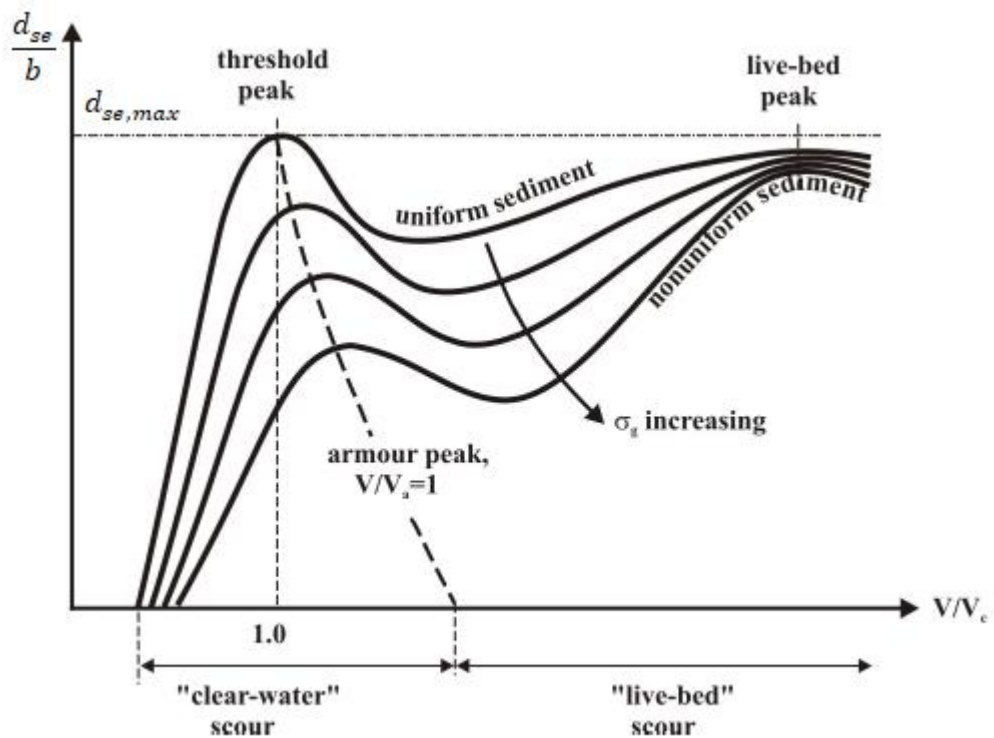
Figure 2.6 The scour depth variation with flow intensity.

When $V/V_c < 0.3 - 0.5$ no scour occurs, the flow velocity is not enough to remove the particles from around the pier.

Under clear-water flow conditions, the scour depth in uniform sediment increases almost linearly with the flow intensity for $(0.3 - 0.5) < V/V_c < 1$. When the flow velocity reaches the threshold velocity of beginning of motion ($V/V_c = 1$), the equilibrium scour depth reaches its maximum, called the threshold peak.

As the velocity exceeds the critical velocity, the local scour depth, first decreases and then increases again to a second peak which corresponds to live-bed conditions.

The second peak is slightly smaller than the threshold peak in uniform sediment. In live-bed conditions, the flow power is consumed both to scour the pier foundation and to transport the sediments [4].

The effect of flow intensity can be obtained by summarizing the result of different investigations [11-15-22].

For calculating the critical velocity, V_c, the following equations are used [22]

$$\frac{V_c}{u_{*c}} = 5.75 \log \left(5.53 \frac{h}{d_{50}} \right) \tag{2.8}$$

where u_{*c} is critical shear velocity given by

$$u_{*c} = 0.0115 + 0.0125 d_{50}^{1.4} \qquad \textit{0.1 mm} < d_{50} < \textit{1 mm} \tag{2.9a}$$

$$u_{*c} = 0.0305 d_{50}^{0.5} - 0.0065 d_{50}^{-1} \qquad \textit{1 mm} < d_{50} < \textit{100 mm} \tag{2.9b}$$

In equations (2.9) u_{*c} is in m/s and d_{50} is in mm.

2.4.6 Effect of time

Time is also an essential parameter of scouring. The time required to sufficiently approach the asymptotic value of the equilibrium scour depth is called time to equilibrium, t_e. Time to equilibrium is different for clear-water and live-bed conditions. Figure 2.7 shows the typical scour depth time evolution for those two situations (clear-water and live-bed condition). In clear-water condition, equilibrium scour depth is reached asymptotically when the flow becomes unable to remove the sediments from the foundation of the bridge pier. Equilibrium scour depth in live-bed condition is reached when the average amount of sediment leaving the scour hole equals the average amount coming in. The equilibrium condition is reached much faster than for clear-water flow condition. The fluctuations around an average value of d_{se} reflects the passage of bed forms.
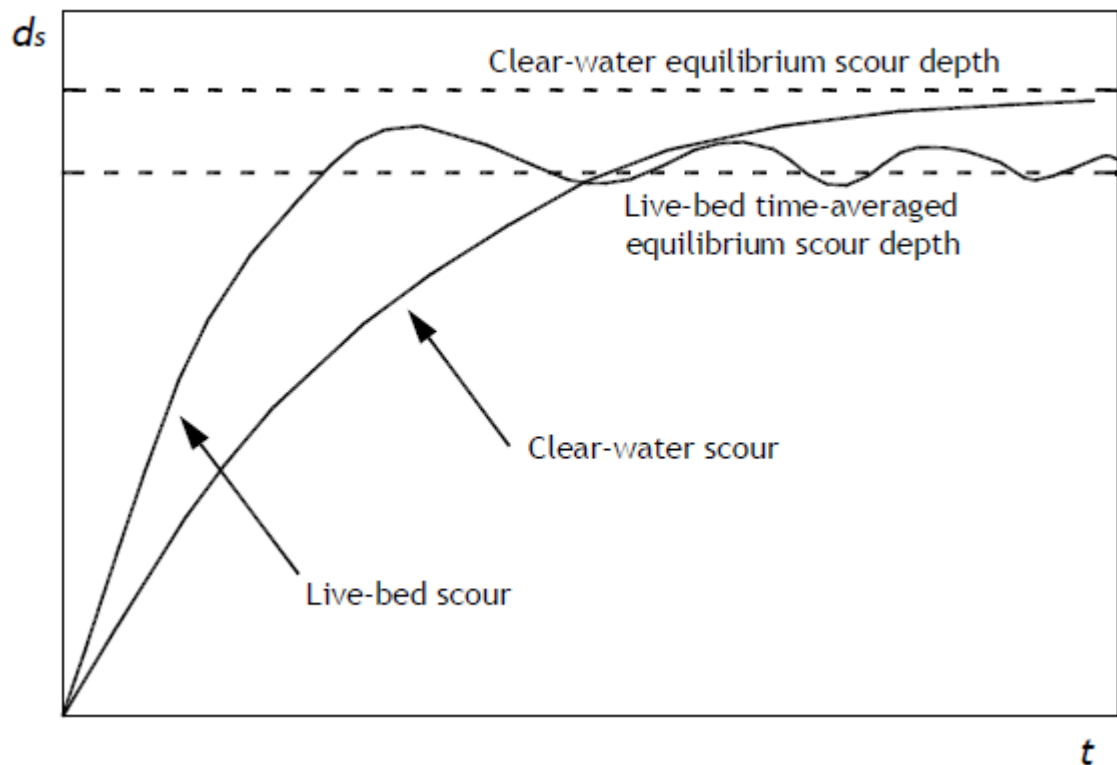
Figure 2.7 Scour depth time development for clear-water and live-bed scour condition, after [28].

It is difficult to materialize the concept of equilibrium in clear-water flow conditions. Ettema (1980) assumed three main phases for the scour process [11].

- Initial phase, down-flow at pier upstream face cause rapid scouring, the horse-shoe vortex does not play a significant role and the sediment transport starts at the sides of the pier.

- The principal phase is dominated by the horse-shoe vortex action; throughout this phase, scour occurs in a narrow strip around the pier. As the scour depth develops the strength of horse-shoe vortex and the down-flow gradually become unable to remove sediment from the entrainment zone.

- The (idealized) equilibrium phase would be reached when no more sediment is transported from the scour hole.

Franzetti et al. (1982) explained equilibrium as a state of scour development where no further change occurs with time. They also mentioned that this condition may take an infinite time to occur [29], meaning that scouring is an asymptotic process.

14

Olivetto and Hager (2002, 2005) also assumed that equilibrium cannot be achieved in finite time and that the scour hole never stops to develop [35].

In practice, Raudkivi (1986) found that 50 hours is enough to reach or to sufficiently approach the equilibrium scour depth in laboratory conditions for clear-water scour [13-4]. Later on, Franzetti et al. (1994) suggested that equilibrium scour at piers is achieved when, $Vt/b > 2 \times 10^6$ [32]. Cardoso and Bettess (1999) proposed that when the slope plot of the scour depth *versus* the logarithm of time changes and tends to zero, then the equilibrium phase is reached [30]. Melville and Chiew (1999) suggested that equilibrium is reached when $\Delta d_S \leq 0.05b/24hr$, which means that when the development of the scour hole is less than 5% of the pier diameter in 24 hours the scour depth is assumed to have reached the equilibrium value [31]. Coleman et al. (2003) pointed out that equilibrium is reached when the scour rate reduces to 5% of the smaller of the flow depth or the foundation length (diameter of the pier or abutment length) in a 24-hour period, *i.e.*, $\Delta d_S \leq 0.05b/24hr$ or $\Delta d_S \leq 0.05h/24hr$ [33]. Mia and Nago (2003) suggested that when the development of scouring is less than 1 mm in one hour, then the experiments can be stopped [34]. Grimaldi (2005) suggested a rather exigent criterion, according to which equilibrium is reached when the scour rate is less than $0.05 \, b/3$ in 24 hours [36]. Fael et al. (2006) have suggested using $2d_{50}$ as the limiting scour increment in 24 hours [37]. More recently, Setia (2008) stated that equilibrium scour could not be reached after more than 100 hours of laboratory experiment [38].

Assuming the asymptotic nature of the scouring process, some other researchers estimate the equilibrium scour depth by extrapolating to infinite time curves adjusted to measured scour depths. One of the curve types is the polynomial function suggested by Bertoldi and Jones (1998) to be presented in section 4.2.3 [55]. In this approach, a key issue is how long the scour depth time records should be to guarantee an accurate value of the equilibrium scour. According to Simarro et al. (2011) the accuracy increases with the length of the records; ideally, the length should be 7 days for single cylindrical piers whereas 4 days guarantee sufficiently robust predictions [56].

2.4.7 Bed material and its effect

The properties of bed material can be defined by its grain size, density and shape. The definition of sediment mixtures further requires the consideration of the gradation coefficient and their cohesive character. The effect of sediment coarseness on scouring was investigated by [11]. The sediment coarseness is defined by Melville and Coleman (2000) as the ratio of the pier diameter, b, to the median grain size, d_{50}, of sediment mixture [22].

Yanmaz (2002) has proposed the equations given below, for the calculation of the sediment coarseness correction factor K_D which is introduced by [4-13]

For $2.9 \leq b/d_{50} < 21$

$$K_D = 1.515 \times 10^{-4} \left(\frac{b}{d_{50}}\right)^3 - 7.53 \times 10^{-3} \left(\frac{b}{d_{50}}\right)^2 + 0.1349 \left(\frac{b}{d_{50}}\right) - 0.0162 \quad \text{(2.10a)}$$

For $21 \leq b/d_{50} < 50$

$$K_D = -8.167 \times 10^{-5} \left(\frac{b}{d_{50}}\right)^2 + 9.247 \times 10^{-3} \left(\frac{b}{d_{50}}\right) + 0.7418 \quad \text{(2.10b)}$$

For $50 \geq b/d_{50}$

$$K_D = 1.0 \quad \text{(2.10c)}$$

This means that, according to Raudkivi (1986), the effect of the grain size would cancel for $b/d_{50} \geq 50$. This result kept undisputed until very recently. Then, Sheppard et al. (2004) and Lee and Sturm (2009) stated that sediment coarseness (b/d_{50}) could induce one of the essential differences between field and laboratory results having an important effect on the scour depth at the prototype scale [39-40].

Recently, after extensive studies on the effect of small sediment coarseness ratios (high values of b/d_{50}) on pier scouring, i.e., studies conducted with the prototype sized piers founded in sandy materials, it was demonstrated that the scour depth reduces significantly for $b/d_{50} > 50$, as shown schematically in Figure 2.8 [31].
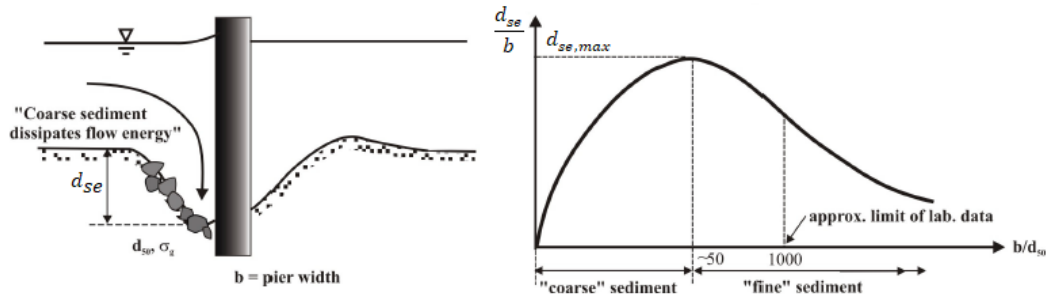
Figure 2.8 Local scour depth variation with sediment coarseness [31].

2.5 Equations for the Local Scour Depth

Many scour predictors can be found in the literature to calculate the local scour depth. Among them, the most up to date predictor based on the equation of Colorado State University (CSU equation) is currently used in U.S Federal High Highway Administration (FHWA), Hydraulic Engineering Circular Number 18 (HEC-18). The predictor of the School of Auckland, initiated by [15] and consolidated by Melville (1997) and Melville and Coleman (2000) have attained a high level of international notoriety. The findings of Florida University, namely those of Sheppard et al. (2004) also deserve a special reference. Next, some of the existing predictors are presented.

2.5.1 Laursen (1958)

Laursen (1958) proposed the following relationship to calculate the maximum scour depth, d_{sm}, at a circular pier under the clear-water condition [41].

$$d_{sm} = 1.34 \left(\frac{h}{b}\right)^{0.5} b \qquad (2.11)$$

2.5.2 Hancu (1971)

Hancu (1971) suggested the following relationship to calculate the final scour depth, d_{sf}, at a circular bridge pier under the clear-water condition [42].

$$d_{sf} = 2.42 \left(\frac{h}{b}\right)^{1/3} Fr^{2/3} b \qquad (2.12)$$

Where Fr is the Froude Number defined as

$$Fr = \frac{V}{\sqrt{gh}} \qquad (2.13)$$

17

2.5.3 Breusers (1977)

Breusers (1977) proposed the following maximum scour depth, d_{sm}, equation [15].

$$d_{sm} = f_1\left\{\frac{V}{V_c}\right\}\left[2.0\tanh\left(\frac{h}{b}\right)\right]K_s\,K_\alpha\,b \qquad (2.14)$$

The term $f_1\left\{\frac{V}{V_c}\right\}$, which is a function of V/V_c, can be calculated by as follows:

$$f_1\left\{\frac{V}{V_c}\right\} = 0 \quad for \quad \frac{V}{V_c} \le 0.5 \qquad (2.15a)$$

$$f_1\left\{\frac{V}{V_c}\right\} = 2\frac{V}{V_c} - 1 \quad for \quad 0.5 < \frac{V}{V_c} > 1 \qquad (2.15b)$$

$$f_1\left\{\frac{V}{V_c}\right\} = 1 \quad for \quad \frac{V}{V_c} > 1 \qquad (2.15c)$$

For circular piers, the shape factor, K_s, and the factor of the angle of attack, K_α, become 1.0.

2.5.4 Jain and Fischer (1979)

Jain and Fischer (1979) have studied the maximum scour depth, d_{sm}, for large Froude numbers in the laboratory and suggested the following equation that includes the critical Froude number, Fr_{crit}, corresponding to the threshold condition of beginning of motion [43].

$$d_{sm} = 1.84\,(Fr_{crit})^{0.25}\left(\frac{h}{b}\right)^{0.3}b \; for \; (Fr - Fr_{crit}) \le 0.2 \qquad (2.16)$$

where the critical Froude number can be calculated as

$$Fr_{Crit} = \frac{V_c}{\sqrt{gh}} \qquad (2.17)$$

2.5.5 Citale (1981)

Citale (1981) proposed an equilibrium scour depth, d_{se}, equation for clear-water condition based only dependent on the pier diameter [44].

$$d_{se} = 2.5\,b \qquad (2.18)$$

2.5.6 Colorado State University (CSU) Equation (1988)

The CSU-Equation (1988) includes K factors to calculate the equilibrium scour depth, d_{se} [46]. This equation is suggested by the Federal Highway Administration in the United States of America [47].

$$d_{se} = 2.0\, K_s\, K_b\, K_\alpha\, K_w \left(\frac{h}{b}\right)^{0.35} Fr^{0.43}\, b \qquad (2.19)$$

Herein, K_s is the pier shape factor. It is assumed to be 1.0 for circular and round-nosed shapes and 1.1 and 0.9 for squared-nosed and sharp-nosed shapes, respectively.

The correction factor associated with the bed forms, K_b, can be determined according to Table 2.3.

Table 2.3 Bed forms correction factor, K_b.

BED CONDITION	DUNE HEIGHT H_d (m)	K_b
Clear-water scour	-	1.1
Plane bed and antidune flow	-	1.1
Small dunes	$0.6 \leq H_d \leq 3$	1.1
Medium dunes	$3 \leq H_d \leq 9$	1.1 to 1.2
Large dunes	$9 \leq H_d$	1.3

The factor of the angle of attack between approaching flow and bridges axis, K_α, become 1.0 for circular piers.

K_w is a for the pier width factor. For wide piers, K_w is equal to 1. Else, if $h/b < 0.8$, $b/d_{50} > 50$ and the flow is subcritical, the value of K_w can be calculated by the equation below.

$$K_w = 2.58 \left(\frac{h}{b}\right)^{0.34} Fr^{0.65} \qquad (2.20)$$

2.5.7 Johnson (1992)

According to Johnson (1992), hydraulic variables such as the discharge, flow depth and velocity are to be considered as stochastic in nature. For this reason, he also claimed that the scour depth itself is a stochastic variable. Therefore, he has followed a probabilistic approach of the pier scour and derived the equilibrium scour depth, d_{se} [46], as given bellow.

$$d_{se} = 2.02\, h\, \left(\frac{b}{h}\right)^{0.98} Fr^{0.21}\ \sigma_g^{-0.24} \tag{2.21}$$

2.5.8 Gao (1993)

Gao (1993) proposed an equation for equilibrium scour depth, d_{se}, based on laboratory studies and a significant number of field data. The advantage of this equation is that it is used for both live-bed and clear-water scour [48]. Moreover, this equation has been used by highway and railway Engineers in China for more than 20 years. It reads

$$d_{se} = 0.46\, K_s\, b^{0.6}\, h^{0.15}\, d_{50}^{-0.07} \left(\frac{V - V_{ic}}{V_c - V_{ic}}\right)^{\eta} \tag{2.22}$$

In the above equation, the correction factor for pier shape, K_s, is 1.0 for circular piers and η is 1.0 for clear-water conditions. V_{ic} is given as

$$V_{ic} = 0.645 \left(\frac{d_{50}}{b}\right)^{0.053} V_c \tag{2.23}$$

2.5.9 Melville (1997)

Melville (1997) proposed the following equation for calculating the equilibrium local scour depth, d_{se} at bridge piers [49].

$$d_{se} = K_{yb}\, K_I\, K_D\, K_S\, K_\alpha \tag{2.24}$$

The depth dimension factor K_{yb}, in deep-water flow ($b/h<0.7$), the K_{yb} is proportional to the pier diameter. In shallow-water depth ($b/h>5$), the scour depth increases linearly with the flow depth. Thus, the scour development is dependent on both flow depth and pier width.

$$K_{yb} = 2.4b \quad for \quad 0.7 < \frac{b}{h} \qquad \text{(2.25a)}$$

$$K_{yb} = 2\sqrt{h\,b} \qquad for \qquad 0.7 \le \frac{b}{h} \le 5 \qquad \text{(2.25b)}$$

$$K_{yb} = 4.5h \quad for \qquad \frac{b}{h} > 5 \qquad \text{(2.25c)}$$

K_I is the flow intensity factor and it takes different values for clear-water and live-bed conditions. For clear-water, $K_I = 2.4\,V/V_c$; for live-bed, $K_I = 1.0$.

By using the following simple equations, the particle size factor, K_D, is calculate

$$K_D = 1 \qquad for \qquad \frac{b}{d_{50}} > 25 \qquad \text{(2.26a)}$$

$$K_D = 0.57\,log\left(2.24\,\frac{b}{d_{50}}\right) \qquad for \qquad \frac{b}{d_{50}} \le 25 \qquad \text{(2.26b)}$$

K_s is the shape factor, which is 1.0 for circular and 1.1 for the square pier. K_α is 1.0 for single cylindrical piers irrespective of α.

2.5.10 May (2002)

May (2002) combined the main results of the approach developed by the different authors such [15-21-12] and proposed the following equation to estimate the equilibrium scour depth, d_{se}:

$$d_{se} = S_F\,K_{yb}\,K_I\,K_S\,K_\alpha\,b \qquad \text{(2.27)}$$

Here SF is the safety factor given in Table 2.4, suggested by Johnson (1992), as a function of the percent number of cases in which the predicted scour depth might be expected to be exceeded [41].

21

Table 2.4 Value of S_F factor.

PERCENTAGE NUMBER OF CASES	S_F
50	1
10	1.20
1	1.40
0.1	1.60
0.01	1.75
0.001	1.85

The effect of the relative water depth, K_{yb}, on the scour depth is calculated with the following relation.

$$K_{yb} = 0.55 \left(\frac{h}{b}\right)^{0.6} \quad for \quad \frac{h}{b} \le 2.7 \tag{2.28a}$$

$$K_{yb} = 1 \quad for \quad \frac{h}{b} \ge 2.7 \tag{2.28b}$$

The effect of the flow velocity is described by the factor K_I, flow intensity.

$$K_I = 0 \quad for \quad \frac{V}{V_C} \le 0.375 \tag{2.29a}$$

$$K_I = 1.6\frac{V}{V_C} - 0.6 \quad for \quad 0.375 < \frac{V}{V_C} \le 1 \tag{2.29b}$$

$$K_I = 1 \quad for \quad \frac{V}{Vc} > 1 \tag{2.29c}$$

If V/V_c is more than 3 to 4 and the bed sediments are widely graded, the flow intensity factor reaches the upper limit of 0.9.

The pier shape factor, K_s, is 1.5 for circular piers. For complex piers, with the shape factor should be obtained with the help of physical hydraulic models.

The effect of pier angle K_α on local scour depth is 1.0 for circular piers.

2.5.11 Lança et al. (2013)

Lança et al. (2013) suggested the following upper bound predictor of equilibrium scour depth [50].

$$\frac{d_{se}}{b} = K_h \, K_D \qquad (2.30)$$

Where K_h and K_{d50} are defined as below.

$$K_h = 2.3 \left(\frac{h}{b}\right)^{1/3} \qquad for \qquad 0.5 \le \frac{h}{b} \le 1.45 \qquad (2.31a)$$

$$K_h = 2.6 \qquad for \qquad \frac{h}{b} > 1.45 \qquad (2.31b)$$

$$K_D = 1 \qquad for \quad for \qquad 60 < \frac{b}{d50} \le 100 \qquad (2.32a)$$

$$K_D = 5.8 \left(\frac{b}{d50}\right)^{1/3} \qquad for \qquad 100 < \frac{b}{d50} \le 500 \qquad (2.32b)$$

$$K_D = 0.55 \qquad for \qquad 60 < \frac{b}{d50} \le 100 \qquad (2.32c)$$

2.5.12 Aksoy and Eski (2016)

Aksoy and Eski (2016) obtained an empirical relation to predict the maximum scour depth, $d_{sm,}$, by using the results of 182 experiments available in the literature [51].

$$\frac{d_{sm}}{b} = 1.39 \, F_d{}^{0.77} \left(\frac{h}{b}\right)^{0.036} \left(\frac{b}{d50}\right)^{-0.194} \qquad (2.33)$$

where F_d is the densimetric Froude particle number which can be calculated as follows:

$$F_d = \frac{V}{(g'd_{50})^{1/2}} \qquad (2.34)$$

where the reduced gravitational acceleration, g', is

$$g' = \Delta g \qquad (2.35)$$

and $\Delta = \rho_s - \rho/\rho$.

2.6 Equations for the Time Evolution of Scour Depth

In literature, there are several empirical or semi-empirical formulas for determination of the time evolution of the scour depth which are listed below.

2.6.1 Franzetti et al. (1982)

Franzetti et al. (1982) proposed an exponential function to assess the time evolution of the scour depth at a circular pier [29]. To derive it they have run experiments with a cohesion-less material whose median size, d_{50}, was 2.13 mm for approach flow velocities in the range $0.13 - 0.19$ m/s. The critical velocity was 0.19 m/s (that mean the flow intensity is $0.68 < V/V_c \leq 1.0$) the tested pier diameters varied between 26.7 and 48 mm. Their functions reads

$$\frac{d_S}{d_{se}} = 1 - \exp\left[a_{1F}\left(\frac{Vt}{b}\right)^{a_{2F}}\right] \tag{2.36}$$

where d_s is the scour depth at any time t and a_{1F} and a_{2F} are constants. These constants were obtained by best fit (least square method) from the experiments performed. Franzetti et al (1982) suggested a_{1F}=-0.028 and a_{2F}=1/3 [26].

2.6.2 Melville and Chiew (1999).

Melville and Chiew (1999) proposed a time-dependent scour depth relationship after using 84 datasets from three different researchers' laboratory data, where flow intensity ranges from 0.46 to 0.957 [31].

$$\frac{d_s}{d_{se}} = exp\left(-0.03\left|\frac{V_c}{V}ln\left(\frac{t}{t_e}\right)\right|^{1.6}\right) \tag{2.37}$$

They also proposed an equation for computing time to equilibrium, t_e, in terms of days of scour processes:

$$t_e = 48.26\frac{b}{V}\left(\frac{V}{V_c} - 0.4\right) \quad for \quad \frac{h}{b} > 6 \tag{2.38a}$$

$$t_e = 30.89\frac{b}{V}\left(\frac{V}{V_c} - 0.4\right)\left(\frac{h}{b}\right) \quad for \quad \frac{h}{b} < 6 \tag{2.38b}$$

2.6.3 Oliveto and Hager (2002)

Oliveto and Hager (2002) proposed a relationship for the computation of the scour depth at a given time, d_s, as a function of time t. This equation is valid for circular piers and rectangular abutments assuming that $h/d_{50} > 5 - 10$. [35]. It reads

- Channel must be almost rectangular in section and straight in the plan.

- Circular or rectangular abutments.
- The fluid is water.
- Flow condition remains constant with time, i. e, steady flow.
- Bed material sediment diameter must be smaller than 5-10 times the flow depth.

$$\frac{d_s}{Z_R} = 0.068N \; \sigma_g^{-\frac{1}{2}} \; F_d^{1.5} log(T) \quad for \; F_d > F_{di} \tag{2.39}$$

where the reference length $Z_R = (hb^2)^{1/3}$, N is as a shape number equal to N=1 for the circular pier and N=1.25 for the rectangular abutment (or pier) and F_d is the densimetric particle Froude number, defined by equation (2.33)

F_{di} is the inception densimetric particle Froude number of sediment movement which can be calculated as;

$$F_{di} = 2.33 \; D_*^{-0.25} \left(\frac{R_h}{d_{50}}\right)^{1/6} \quad for \qquad D_* \leq 10 \qquad \text{(2.40a)}$$

$$F_{di} = 1.08 \; D_*^{1/12} \left(\frac{R_h}{d_{50}}\right)^{1/6} \qquad for \quad 10 < D_* < 150 \quad \text{(2.40b)}$$

$$F_{di} = 1.65 \left(\frac{R_h}{d_{50}}\right)^{1/6} \qquad for \quad D_* \geq 10 \qquad \text{(2.40c)}$$

Herein D_* is the dimensionless grain size defined as $D_* = \left(\frac{g'}{v^2}\right)^{1/3} d_{50}$. The dimensionless time of scouring is defined by $T = \frac{t}{t_R}$, where

$$t_R = \frac{Z_R}{\left[\sigma_g^{1/3} (g'd_{50})^{0.5}\right]} \tag{2.41}$$

2.6.4 Kothyari et al. (2007)

After the study of [35], Kothyari et al. (2007) claimed that it is more realistic to relate the depth of the scour at circular bridge piers to the difference between actual densimetric particle Froude number, F_d and the entrainment densimetric particle Froude number, $F_{d\beta}$ [53]. They supported this concept by studying the variation of scour depth with time for different values of (F_d- $F_{d\beta}$) considering a significant volume of data from various studies.

They conducted an experimental series for calculating the temporal evolution and the maximum scour depth under both clear-water and live-bed condition [53]. All the experiments were carried out in a 30 m long, 1 m wide and 0.6 m deep fixed bed masonry flume and four different uniform sediments having the median diameters of 0.41 mm, 0.50 mm, 0.71 mm and 0.88 mm; they have used circular cylindrical galvanized iron pipes having the diameters of 6.5 cm, 11.5 cm and 17 cm as bridge pier models.

The relationships derived by them for the determination of temporal variation of scour around a circular bridge pier is given below.

$$\frac{d_S}{Z_R} = 0.272 \, \sigma^{-1/2} \, (F_d - F_{d\beta})^{2/3} \log T \tag{2.42}$$

where $F_{d\beta}$ is calculated as follows:

$$F_{d\beta} = \left[F_{di} - 1.26 \, \beta^{0.24} \left(\frac{R_h}{d_{50}} \right)^{\frac{1}{6}} \right] \sigma^{\frac{1}{3}} \tag{2.43}$$

In this equation $\beta = b/B$, R_h is the hydraulic radius and $F_{di,}$ is inception densimetric particle Froude number of sediment movement, defined by equation 2.40.

2.6.5 Lança et al. (2013)

Lança et al. (2013) carried out long scour duration experiments around circular bridge piers under the clear-water condition where the average flow intensity was $0.93 < V/V_c \leq 1.04$ and proposed a time-dependent scour depth equation as given below [50].

$$\frac{d_s}{d_{se}} = 1 - \exp \left[-a_{1L} \left(\frac{Vt}{b} \right)^{a_{2L}} \right] \tag{2.44}$$

where $a_{1L} = 1.22 \left(\frac{b}{d_{50}} \right)^{-0.764}$ and $a_{2L} = 0.09 \left(\frac{b}{d_{50}} \right)^{0.244}$

They also investigated the effect of sediment coarseness b/d_{50} on the equilibrium scour depth and provided the following relation.

$$\frac{d_{se}}{b} = 7.3 \left(\frac{b}{d_{50}}\right)^{-0.29} \left(\frac{h}{b}\right)^{0.12} \quad for \quad 60 \leq \frac{b}{d_{50}} \leq 500 \qquad (2.45a)$$

$$\frac{d_{se}}{b} = 1.2 \left(\frac{h}{b}\right)^{0.12} \quad for \quad \frac{b}{d_{50}} > 500 \qquad (2.45b)$$

2.6.6 Aksoy et al. (2017)

Aksoy et al. (2017) also suggested an empirical equation, after conducting experiments in an 18.6 m long and 0.80 m wide rectangular flume with a 0.006 bed slope. They have used uniform gravel bed material (median diameter of 3.5 mm) [54] and tested diameters of the circular piers equal to 40 mm, 80 mm, 150 mm and 200 mm subjected to four different steady discharges (52 l/s, 56 l/s, 61 l/s and 66 l/s) where the flow intensity is $0.48 < V/V_c \leq 0.55$. Their equation reads

$$\frac{d_s}{b} = 0.8 \left(\frac{V}{V_c}\right)^{1.5} \left(\frac{h}{b}\right)^{0.15} (log \, T_s)^{0.6} \qquad (2.46)$$

in which $T_{s,}$ is a dimensionless time parameter which can be expressed as follows (Yanmaz and Altınbilek, 1991)

$$T_s = t \frac{d_{50}(\Delta \, g \, d_{50})^{0.5}}{b^2} \qquad (2.47)$$

3. EXPERIMENTAL SET-UP

3.1 Experimental Set-up

The experiments were conducted in 18 m long and 1.49 m height rectangular channel made from concrete located at Hydraulic Laboratory of İzmir Kâtip Çelebi University in the Department of Civil Engineering (Figure 3.1). The sidewalls of the channels are made of concrete, which are 2 m apart from each other. A sketch of the experimental set-up is given in Figure 3.2.

Figure 3.1 View of the experimental set-up.
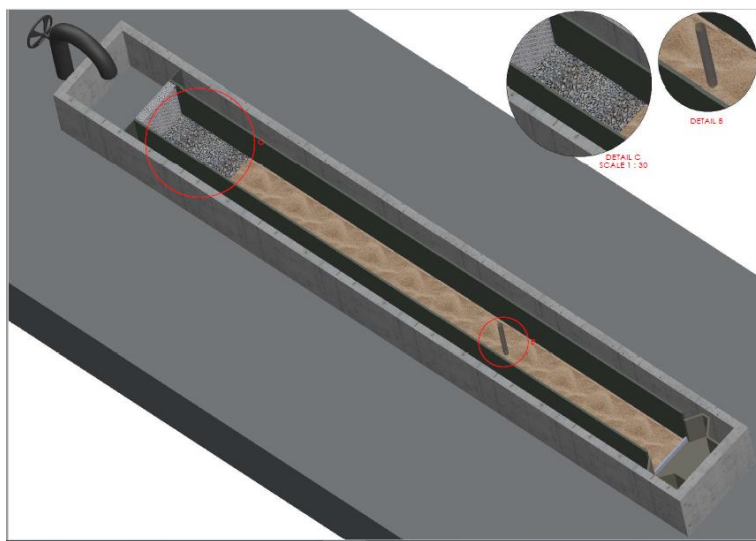
Figure 3.2 A sketch of the experimental set-up.

The experiments were carried out for three different widths of the channel. In order to change the width of the channel to 177 cm, 120 cm and 74 cm, two metallic side walls were inserted inside the concrete channel (Figure 3.3 - 3.4). The net length of the channel was 15 m, excluding the 190 cm entrance and 130 cm exit parts.
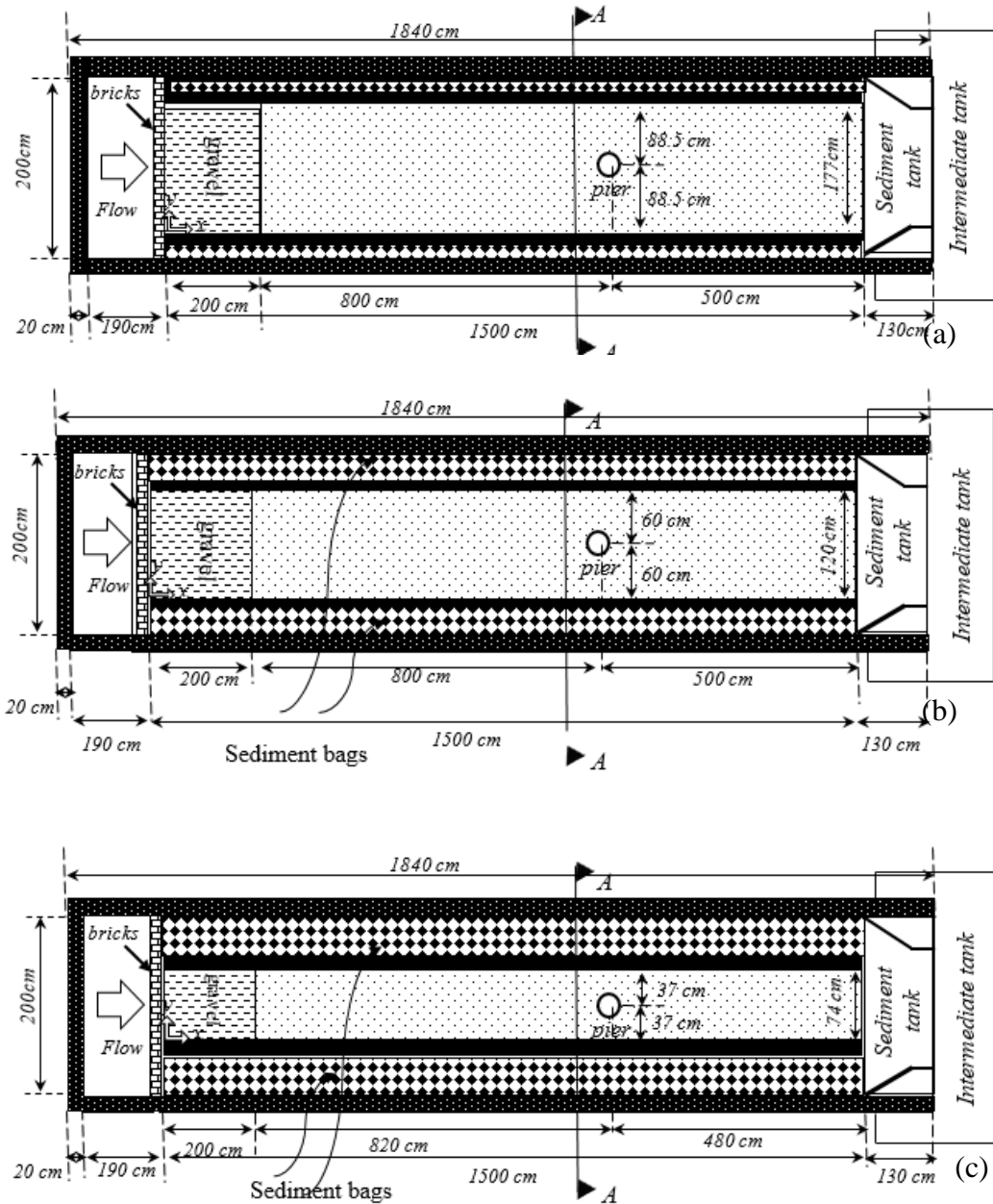
Figure 3.3 The plan view of the channel, (a) 180 cm width (wide channel), (b) 120 cm width (c) 70 cm width (narrow channel).
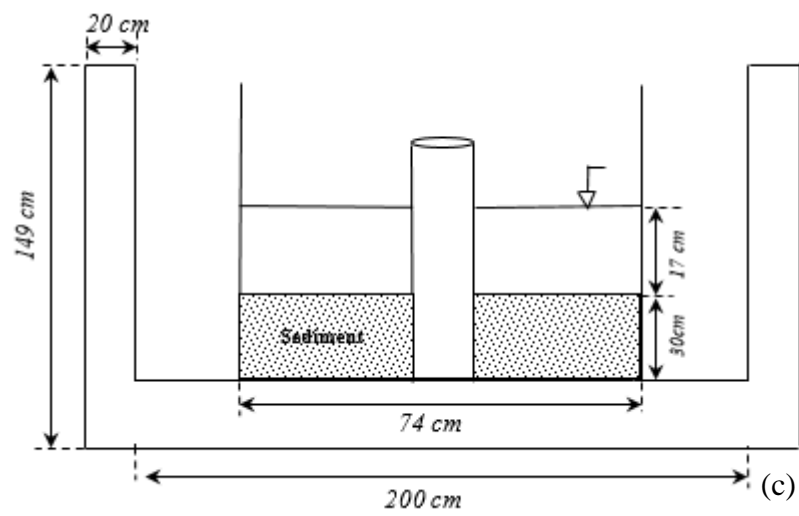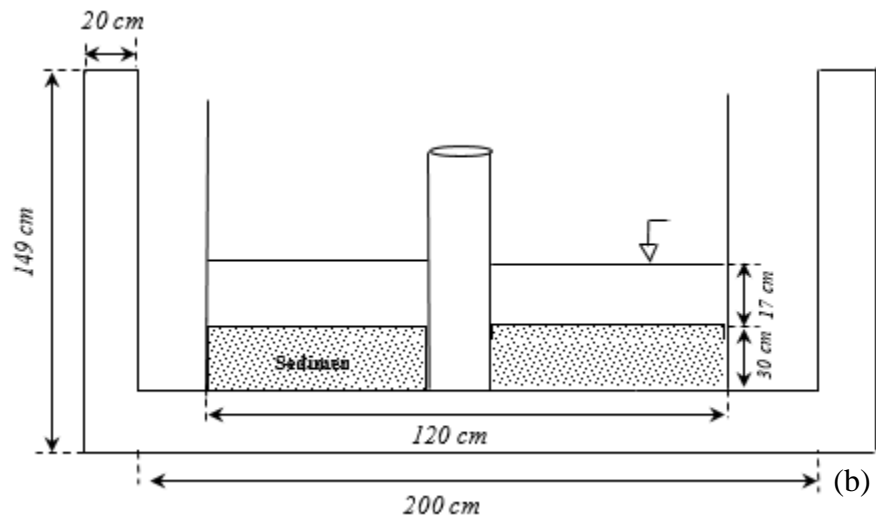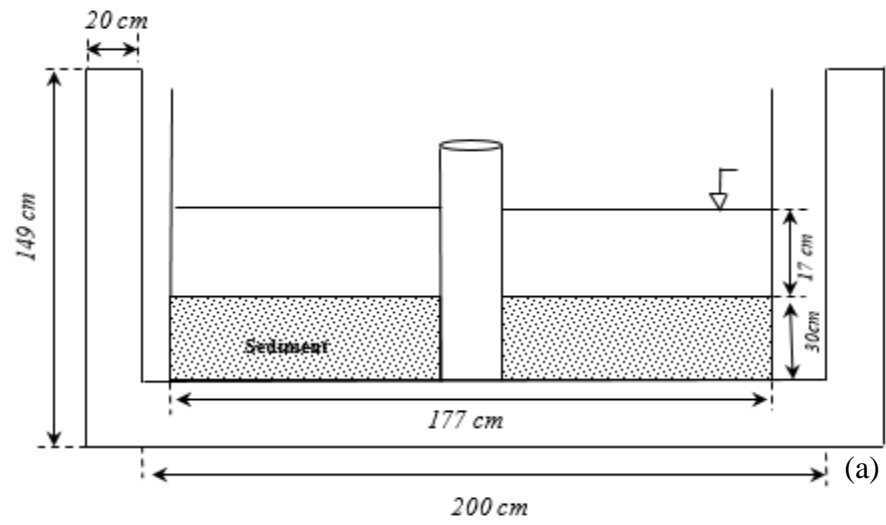
Figure 3.4 The cross section A-A give in the plan view of channel (a) 180 cm width, (b) 120 cm width, (c) 70 cm width.

The channel bed was covered with a sediment layer whose thickness was 30 cm. The upstream 2 m long reach of the channel floor was covered with coarse gravel to induce the development of fully turbulent flow and prevent local scouring at the channel entrance (Figure 3.5).

Figure 3.5 Coarse gravel at upstream of the channel.

Three clear Plexiglas cylindrical piers with diameters equal to 0.07 m, 0.12 m and 0.16 m were utilized. Inside the piers, a transparent scale was inserted at 180º and 0º angles marked upstream and downstream face of the pier, respectively. Circular piers were selected because of their symmetry and the abundance of data available for comparative purposes. All three piers were placed at the centre line of the channel for each experiment. In the longitudinal direction, the piers were placed at 8 m from the gravel reach (10 m from the channel entrance).
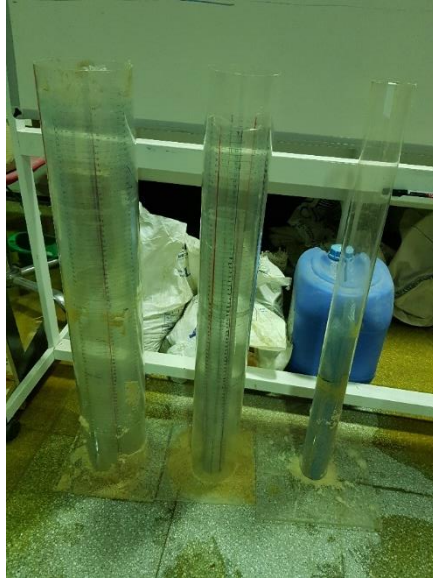
Figure 3.6 Bridge pier of diameter 16 cm, 12 cm and 7 cm.

In order to level the bed of the channel, a horizontal transverse bar was attached to a car that moved along the channel (Figure 3.7).

Figure 3.7 Apparatus to level the channel bed along the channel.

To supply water to the channel, there is a reservoir with a capacity of 24 m^3 (Figure 3.8). An electromagnetic flow-meter is placed on the inlet pipe (see section 3.3.1). The water flows from the reservoir to the flume by the action of a centrifugal pump with 15 KW power (Figure 3.9) installed in the basement of the laboratory.

Figure 3.8 Main reservoir.

Figure 3.9 Centrifugal pump.

3.2 Bed Material Characteristics

Uniform sand was used as bed sediments. Before and after the first experiment, four different samples were collected from different locations along the channel and the sieve analysis was performed. The d_5, d_{10}, d_{50}, d_{60} and d_{95} values are the grain sizes corresponding to 5%, 10%, 50%, 60% and 95% of the cumulative grain size distribution curve by weight, d_g is the geometric mean size and σ_g is the gradation coefficient. These values are listed in Table 3.1. The complete gradation curve is shown in Figure 3.10 [8].

Table 3.1 Sediment properties [8].

GRAIN SIZE	SAMPLE 1	SAMPLE 2	SAMPLE 3	SAMPLE 4	AVERAGE
D_5	0.716	0.767	0.744	0.762	0.744
D_{10}	0.851	0.868	0.860	0.866	0.861
D_{50}	1.036	1.051	1.042	1.047	1.044
D_{60}	1.065	1.077	1.070	1.075	1.072
D_{95}	1.172	1.174	1.175	1.176	1.174
d_g	1.005	1.025	1.017	1.024	1.018
σ_g	1.160	1.149	1.166	1.166	1.160
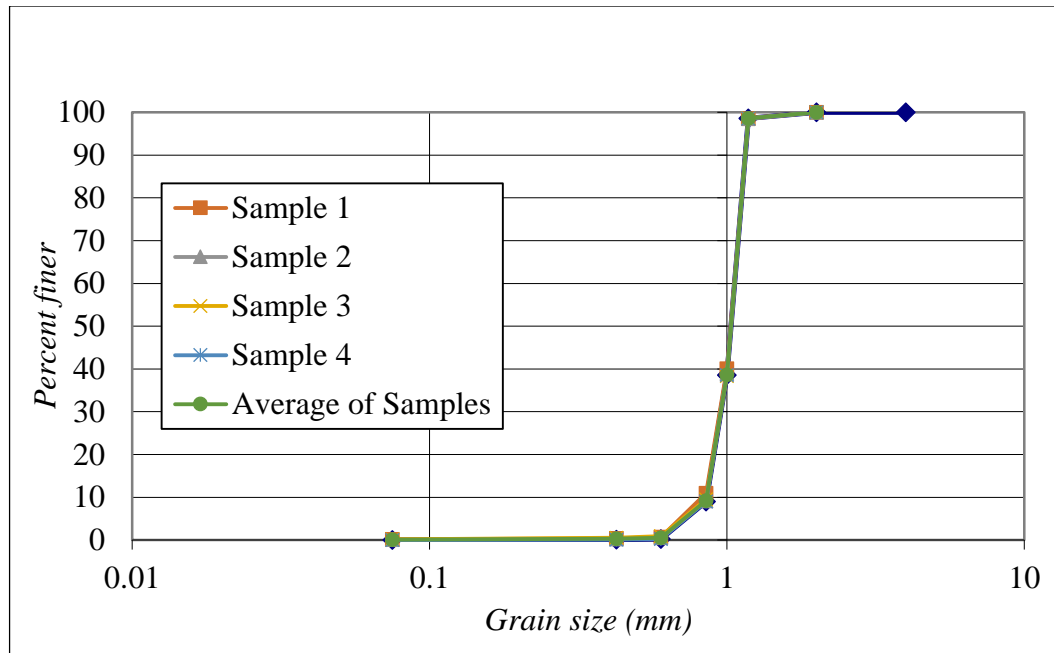
Figure 3.10 Particle size distribution of the bed material [8].

As it is seen in the Table 3.1, the gradation coefficient of the bed material is $\sigma_g = 1.16$, smaller than 1.3, which means that the sediment distribution can be considered as uniform according to [4].

3.3 Instrumentation

3.3.1 Flow-meter

An electromagnetic flow-meter (OPTIFUX 1000 By Krohne) was used to measure the discharge; it is installed on the main supply pipe upstream of the channel entrance; it measures the flow rate with 0.1 l/s precision (Figure 3.11).
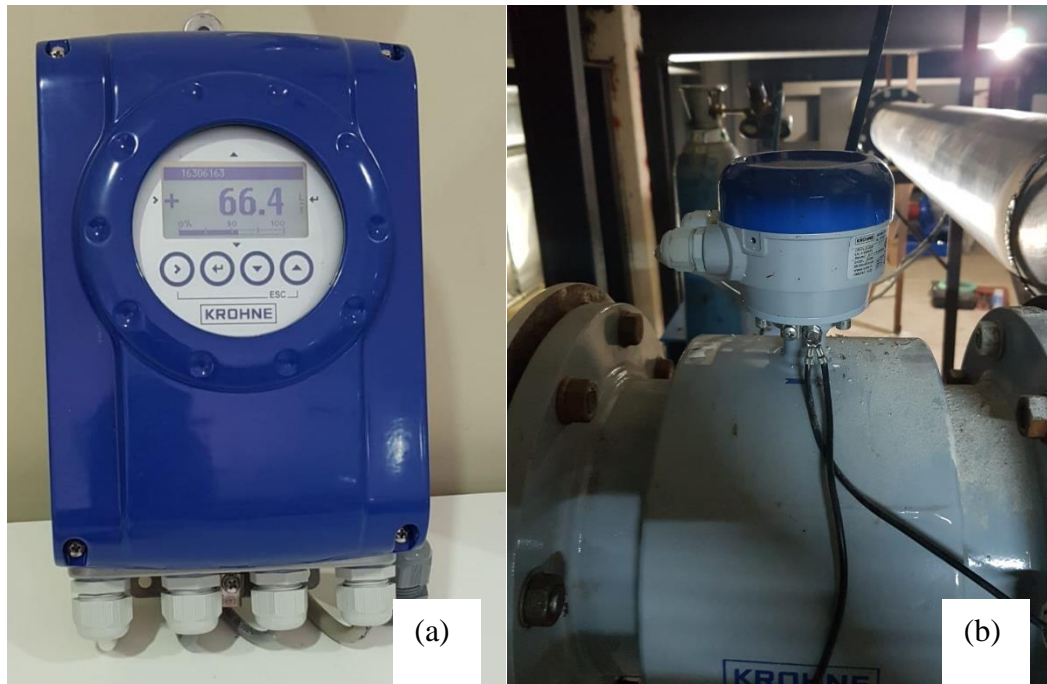
Figure 3.11(a) and (b) Flow meter OPTIFUX 1000

3.3.2 Programmable logic controller (PLC)

To adjust or change the discharge, a PLC board was used (Figure 3.12). The maximum and minimum values of PLC are 50 HZ and 0 HZ with a precision of 0.1 HZ and PLC has a control unite. Then, the PLC board is changed to on automatic system that records the discharge (Figure 3.13).
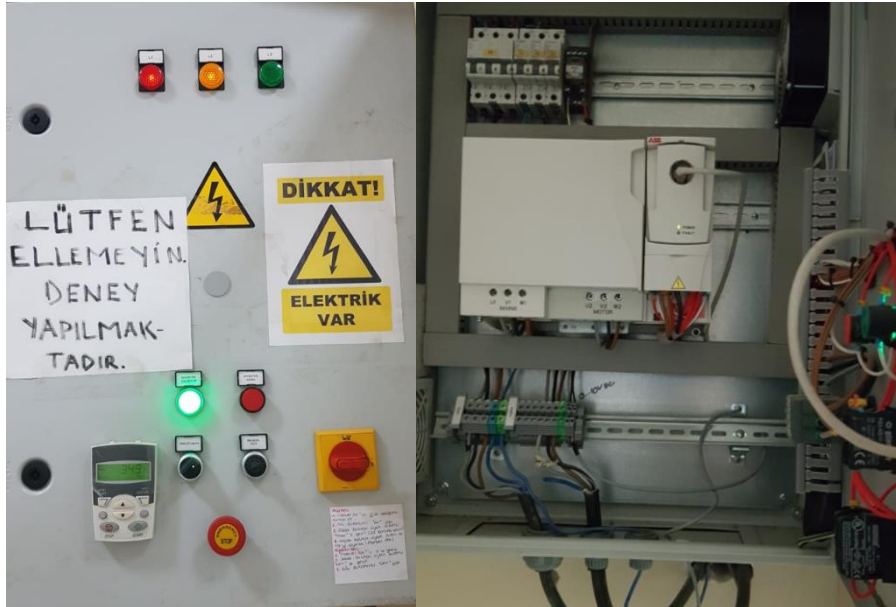
Figure 3.12 PLC device
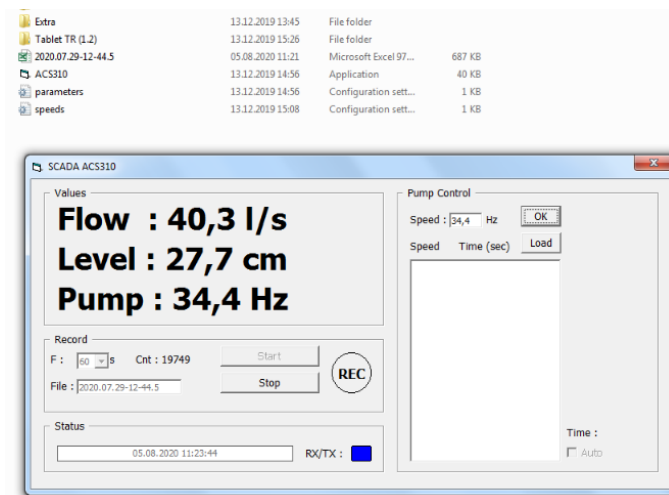
Figure 3.13 Automatic system

3.3.3 GoPro Camera

To measure the level of the sand, a GoPro camera was used (Figure 3.14). With the starting of the experiments, the sand level evolution was regularly recorded by placing the camera inside the bridge pier (see Figure 3.15). This was done at time intervals that allowed to determine the bed level along time.

Figure 3.14 GoPro camera

elevation of the bed 7.6 cm
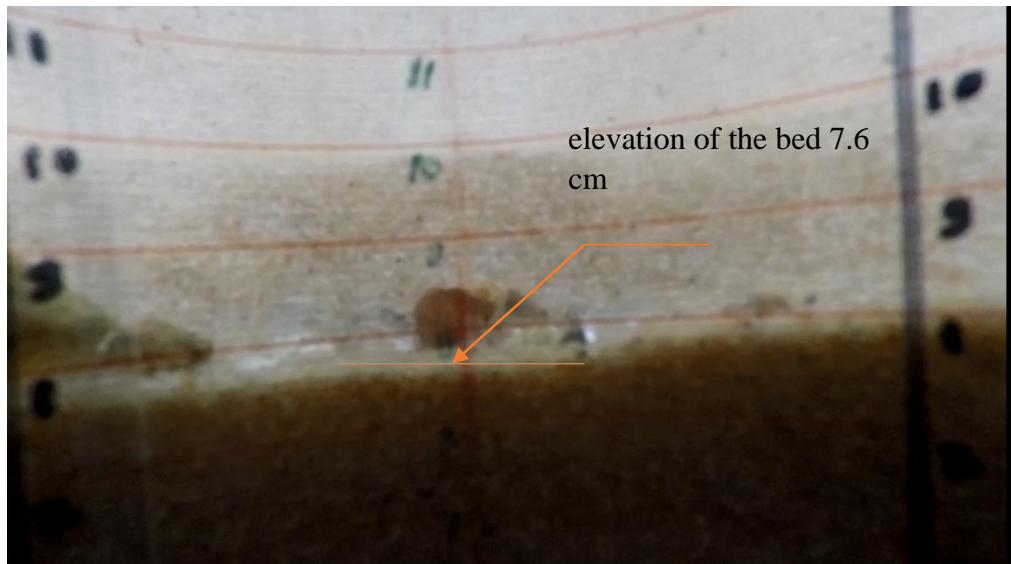
Figure 3.15 The photo showing the view recorded value at the upstream face of the pier.

3.4 Experimental Procedure

Before starting each experiment, the pier was placed, as stated before, at the center of the channel at 10 m from its upstream cross section (Figure 3.16).

Figure 3.16 Pier is placed at the center of the channel.

Prior to each run, the sediment bed was levelled as previously described. Then the pump was turned on. The tail gate was kept closed until the flume was filled with water. Before the gate was opened, the initial scour hole was filled again. ,. Then the gate was slowly opened trying not to move sediments from the bed and to get the desired water depth. The initial time was established and the scour evolution was recorded with the GoPro camera. The pump speed was adjusted to get the desired flow discharge and the flow depth was imposed to be 0.17 m. The first 12 hours of each experiment were the most dynamic. Therefore, the GoPro camera was operated at small intervals to record the bed level. After this period, as the duration of the experiment increased, the data was recorded at increasing time intervals. Finally, the water surface profile was measured along the length of the flume to calculate the water surface slope.

The duration of each experiment was selected to be at least approximately 4 days. At the end of each experiment, the tail-gate was slowly closed and the velocity was decreased to fill the flume without disturbance. The pump was slowly closed. Then, the water was slowly drained and pictures were taken. Then, the channel was prepared for next experiment.

In this study, 5 experiments were conducted for two different channel widths: narrow (n; 74 cm) and wide (w; 177 cm).

The data of 3 experiments by Kılınç (2019) were also used since they were obtained in the same installation with the same procedure [8]. Kılınç's channel width was 120 cm and other parameters were the same, the flow intensity was kept almost constant and the same 3 cylindrical pier diameter were used.

Table 3.2 shows the most important control variables and non-dimensional parameters which characterize the experiments. The flow depth and flow discharge were kept practically constant. The bed material was always the same. The Froude number for all the experiments was less the 1, guaranteeing subcritical conditions.

The Reynolds number and pier Reynolds number were calculated by following equations.

$$Re = \frac{4VR_h}{\nu} \tag{3.1}$$

$$Re_{pier} = \frac{Vb}{\nu} \tag{3.2}$$

The name of the each experiment refers, first, the flow intensity: for instance A stands for the flow intensity 0.6. Next, it contains the pier diameter and, finally, it informs on the channel width (n and w correspond to narrow and wide channel, respectively). For instance, A07w corresponds to a 0.6 average flow intensity and a diameter of the pier equal to 7 cm in the wide channel. This is included in a wider project where there were other flow intensities exploited.

Table 3.2 Characteristics values of parameter in the experiments.

EXP	A07w	A12w	A16w	A07	A12	A16	A07n	A12n
Q (l/s)	79.3	79.3	79.3	51.0	51.0	51.0	31.5	31.5
B (m)	1.77	1.77	1.77	1.20	1.20	1.20	0.74	0.74
b (cm)	7.0	12.0	16.0	7.0	12.0	16.0	7.0	12.0
V (m/s)	0.26	0.26	0.26	0.25	0.25	0.25	0.25	0.25
$V_c{}^1$ (m/s)	0.424	0.424	0.424	0.424	0.424	0.424	0.424	0.424
V/V_c	0.62	0.62	0.62	0.59	0.59	0.59	0.59	0.59
t_{dur} (hr)	94.4	97.2	96.0	410.0	262.0	237.0	96.1	96.9
b/d_{50}	67	115	153	67	115	153	67	115
b/B	0.040	0.068	0.090	0.058	0.100	0.133	0.095	0.162
b/h	0.4	0.7	0.9	0.4	0.7	0.9	0.4	0.7
$Re^2 \times 10^5$	1.51	1.51	1.51	1.74	1.74	1.74	1.17	1.17
$Re_{pier}{}^3 \times 10^4$	1.85	3.17	4.23	1.75	3.00	4.00	1.75	3.00
Fr^4	0.205	0.205	0.205	0.194	0.194	0.194	0.194	0.194
$t_R{}^5$	0.69	0.99	1.2	0.69	0.99	1.2	0.69	0.99
$Z_R{}^6$	0.09	0.13	0.16	0.09	0.13	0.16	0.09	0.13
$F_{di}{}^7$	3.22	3.22	3.22	3.18	3.18	3.18	3.11	3.11
$F_d{}^8$	2.03	2.03	2.03	1.92	1.92	1.92	1.93	1.93
$F_{d\beta}{}^9$	2.04	1.85	1.74	1.88	1.67	1.55	1.66	1.43

1: see chapter 2.4.6 and equation (2.8) for critical velocity (V_c).

2: See chapter 3.4 and equation (3.1) for the equation of Reynolds number (Re)

3: See chapter 3.4 and equation (3.2) for the equation of pier Reynolds number (Re_{pier})

4: See chapter 2.5.2 and equation (2.13) for the equation of Froude number (F_r)

5: See chapter 2.6.3 and equation (2.41) for the equation of reference time (t_R)

6: See chapter 2.6.3 and the equation of references length (Z_R)

7: See chapter 2.6.3 and equation (2.40) for the equation of densimetric particle Froude number for the inception of sediment movement in approach flow (F_{di})

8: See chapter 2.5.12 and equation (2.34) for the equation of densimetric Froude number (F_d)

9: See chapter 2.6.4 and equation (2.43) for the equation of densimetric particle Froude number of scour entrainment ($F_{d\beta}$)

4. EXPERIMENTAL RESULTS

4.1 Time Evolution of Maximum Local Scour Depth

The sediment's movement around the pier is promoted mostly by the vortex structure that develops locally in such a way that the particles at the upstream face of the pier are removed and deposited in the downstream of the pier. As stated in the literature and observed in the experiments, the evolution of the scour is very rapid in the first day of the experiments. Large deposits are formed in this period too. When the scour hole enlarges with time, horseshoe vortices lose their strength and the rate of scouring decreases. During the experiments, the maximum scour depth was initially observed in the pier sides and then roamed to the upstream face of the pier. Besides that, the minimum scour depth was observed in downstream face of the pier. For all the experiments, the maximum local scour occurred in front of the pier. The scour depth evolution in this location is given in Figure A1.1 in Appendix I.

4.1.1 Comparison of experimental results with the predictors given for the evolution of local scour

Over the past decades, researchers have provided a number of semi-empirical equations for estimating of the local scour depth at bridge piers. Next, six of the most widely used predictors of the scour depth evolution presented in Chapter 2 were used. The results of this study are compared with those obtained by using the predictors. Figure 4.1 to Figure 4.8 confront the temporal scour depth evolution of all the experiments with the predictions of Franzetti et al. (1982), Melville and Chiew (1999), Oliveto and Hager (2002), Kothyari et al. (2007), Lança et al. (2013) and Aksoy et al. (2017)[29-31-35-53-54].

As it is seen from the figures, the curve representing the predictor of Melville and Chiew (1999) is cut at the time calculated by equation (2.38), which corresponds to their definition of the equilibrium time as summarized in Table 4.1 for all the experiments.

Table 4.1 Time to equilibrium values of the experiments calculate by the method proposed by Melville and Chiew (1999) by equation 2.38

EXP	A07w	A12w	A16w	A07	A12	A16	A07n	A12n
Time to equilibrium (hr) by equation 2.38	54.6	81.8	101.5	47.4	72.9	91.7	50.1	75.1

Time evolution equations proposed by Franzetti et al. (1982), Melville and Chiew (1999) and Lança et al. (2013) require the *a priori* knowledge of equilibrium scour depth, d_{se}, (see equation (2.36), (2.37) and (2.44) respectively). The calculation of equilibrium scour depth in equation (2.36) is made by the criteria described in (2.4.6) by Franzetti et al. (1994) whereas Melville and Chiew (1999) and Lança et al. (2013) proposed a set of equations for the same purpose, namely equations (2.24)-(2.26) and (2.45) respectively.
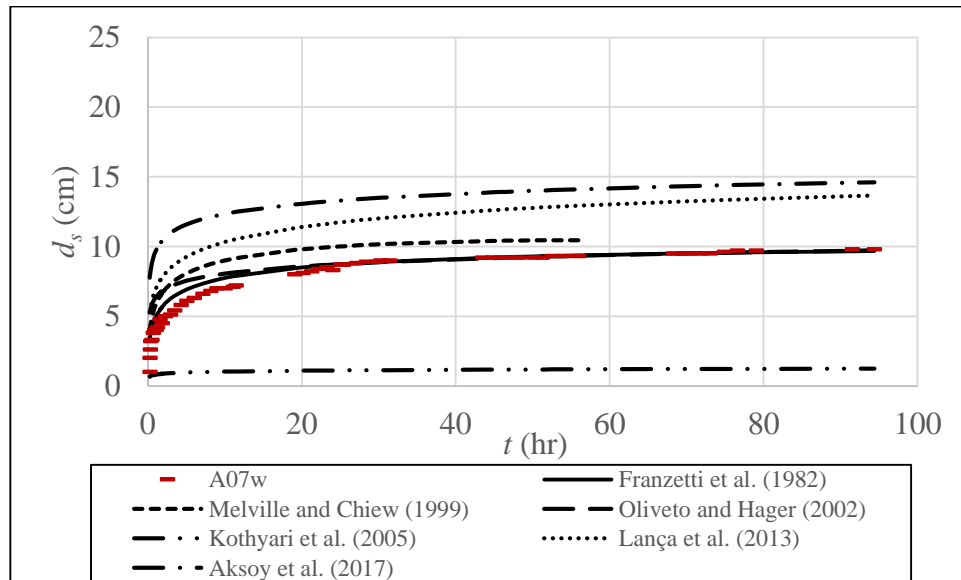

Figure 4.1 The graph of time evolution for A07w.

Figure 4.2 The graph of time evolution for A12w.

Figure 4.3 The graph of time evolution for A16w.
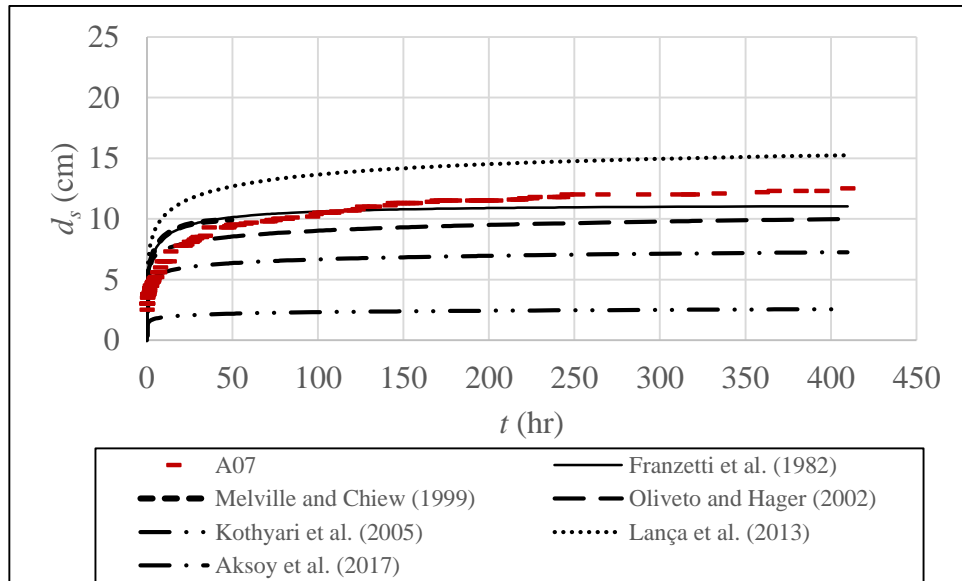
Figure 4.4 The graph of time evolution for A07.
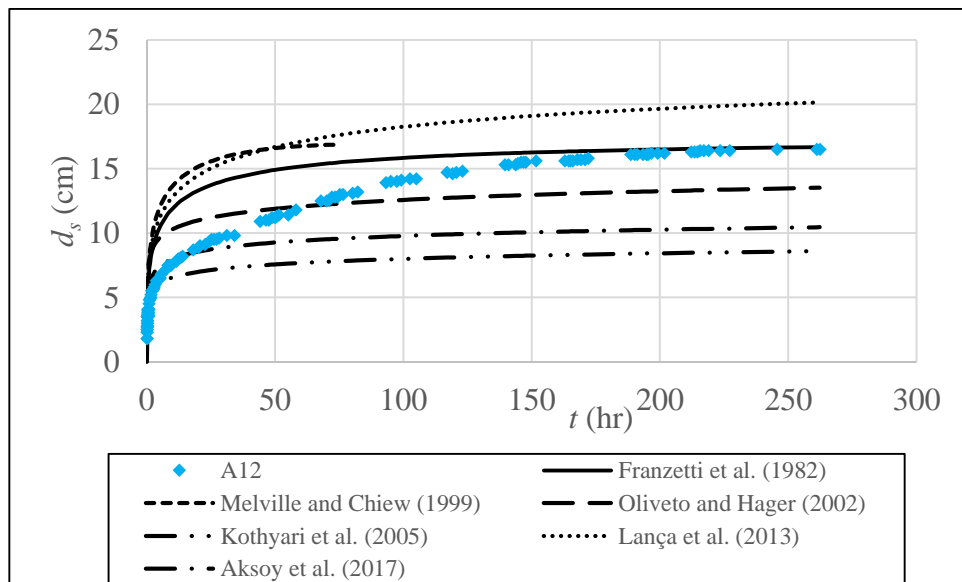
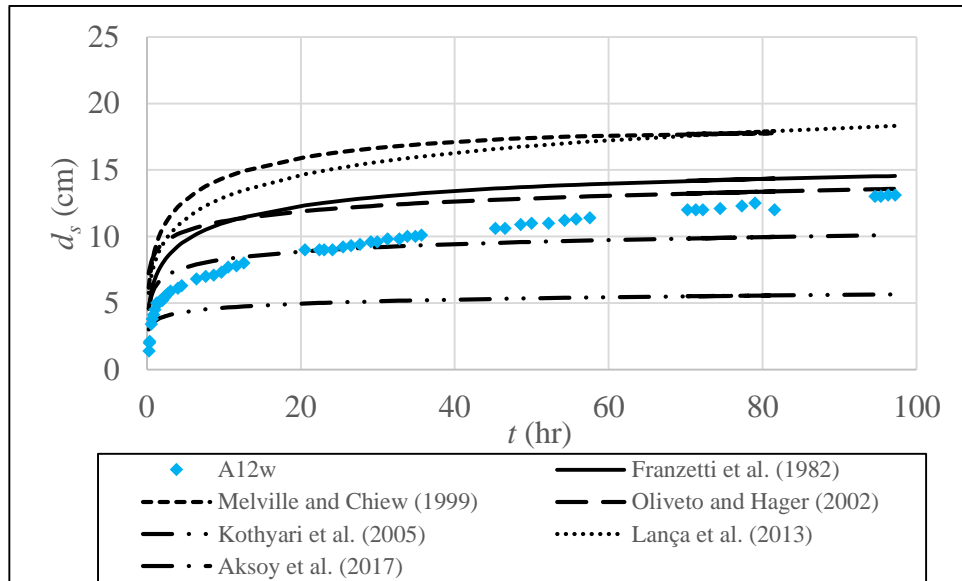**Figure 4.5** The graph of time evolution for A12.

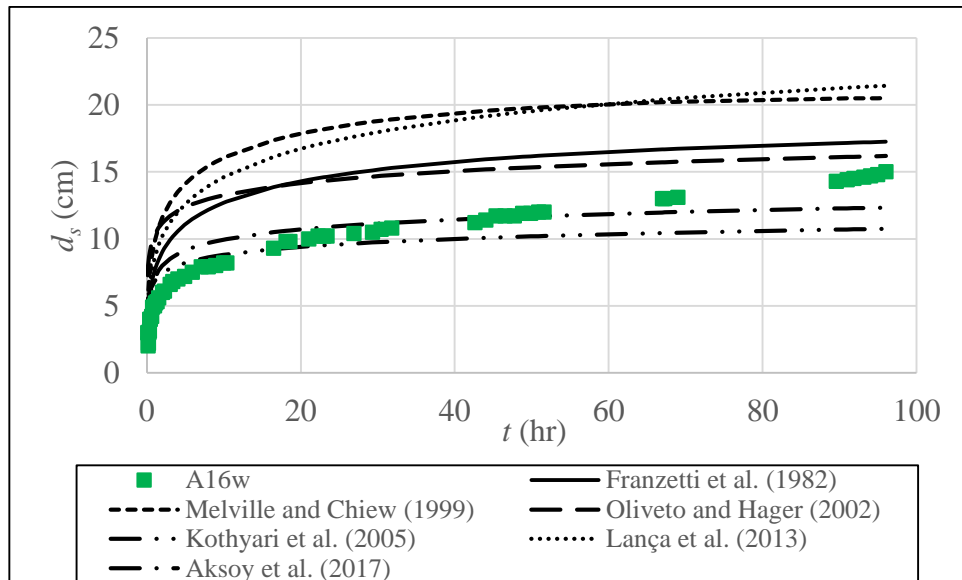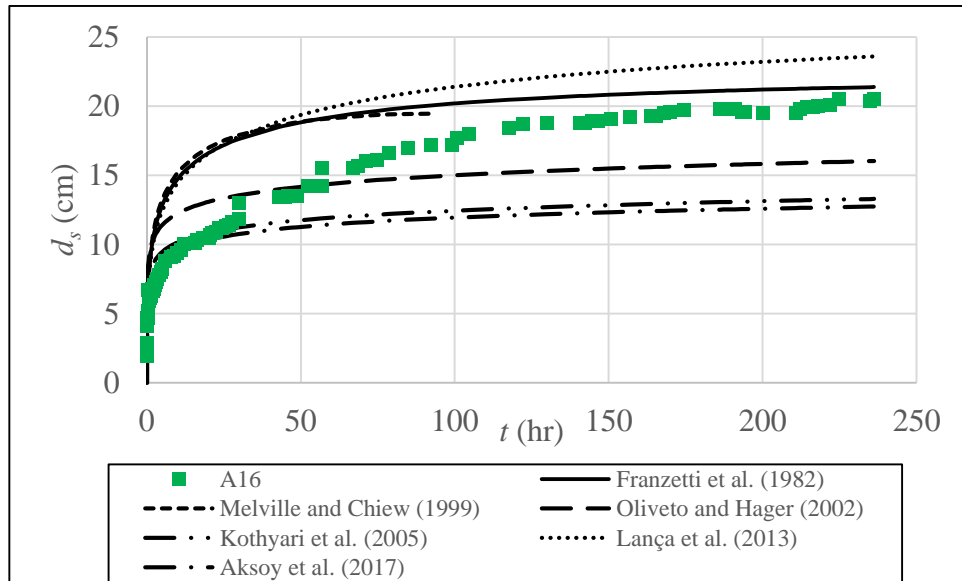**Figure 4.6** The graph of time evolution for A16.
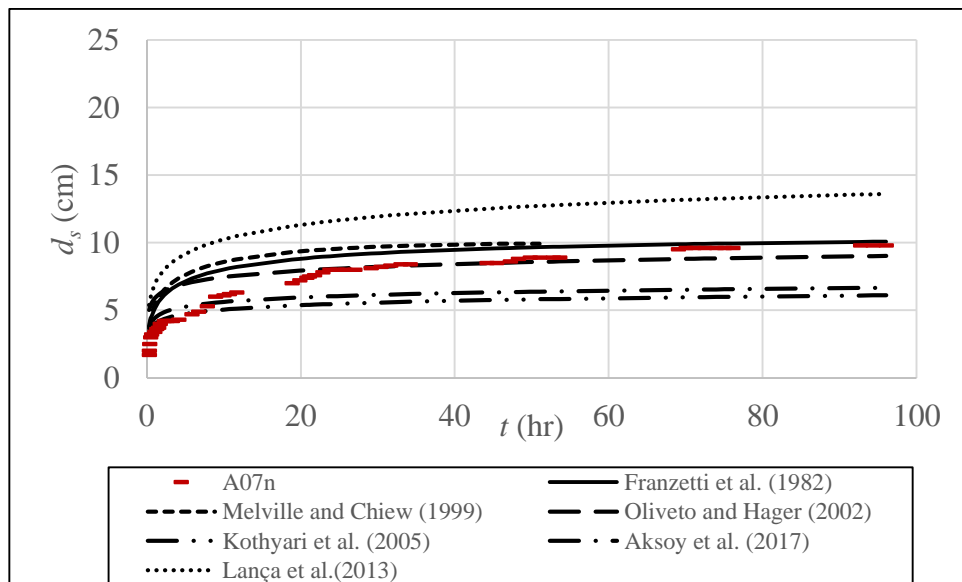
Figure 4.7 The graph of time evolution for A07n.
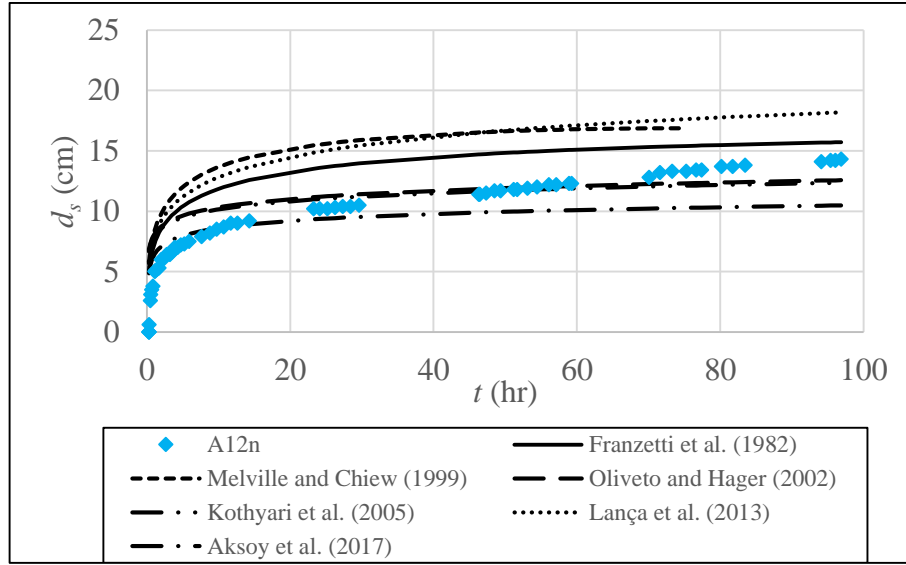
Figure 4.8 The graph of time evolution for A12n.

Root Mean Square Error (RMSE) and Mean Absolute Error (MAE) are the statistics used to evaluate the agreement. The Root Mean Square Error (RMSE) and Mean Absolute Error (MAE) equation are given below, respectively.

$$RMSE = \sqrt{\frac{1}{n}\sum\nolimits_{i=1}^{n}\left(x_{i,est} - x_{i,obt}\right)^2} \qquad (4.1)$$

$$MAE = \frac{1}{n}\sum\nolimits_{i=1}^{n}\left|x_{i,est} - x_{i,obt}\right| \qquad (4.2)$$

In these equations $x_{i,est}$ are the estimated or calculated values and $x_{i,obt}$ are the experimentally obtained or measured values and n is the number of data points.

Both RMSE and MAE are normalized by the measured end scour depth, $d_{s,end}$, of all the experiments. RMSE and MAE are divided by the measured end scour depth and multiply with 100 to get the normalized percent error. The percentage derivations are given in Table 4.2 and Table 4.3, respectively.

Table 4.2 Comparison of experimental and calculated values of, d_s, on the percentage basis of normalized Root Mean Square Error (RMSE) in 100%.

EXP	A07w	A12w	A16w	A07	A12	A16	A07n	A12n	Average
Franzetti et al. (1982)	**7**	21	25	10	15	16	15	22	**16**
Melville and Chiew (1999)	**17**	47	44	26	24	19	21	33	29
Oliveto and Hager (2002)	**14**	24	29	14	16	15	15	18	**18**
Kothyari et al. (2007)	67	34	*13*	65	29	19	24	18	34
Lança et al (2013)	34	40	40	25	23	**17**	39	18	26
Aksoy et al. (2017)	52	**13**	10	27	20	18	20	116	35

Table 4.3 Comparison of experimental and calculated values of, d_s, on the percentage basis of Mean Absolute Error (MAE) 100%.

EXP	A07w	A12w	A16w	A07	A12	A16	A07n	A12n	Aveage
Franzetti et al. (1982)	**4**	21	24	10	12	14	13	21	**15**
Melville and Chiew (1999)	16	46	43	21	22	**15**	20	32	27
Oliveto and Hager (2002)	**9**	22	27	13	15	14	11	14	**16**
Kothyari et al. (2007)	64	29	**11**	60	21	13	21	13	29
Lança et al (2013)	33	40	38	24	22	**14**	39	**14**	25
Aksoy et al. (2017)	52	11	**10**	23	15	17	18	13	20

Analyzing the laboratory data, the best agreement between the predicted and the observed scour depth is given by equations of Franzetti et al. (1982) and Oliveto and Hager (2002).

4.1.2 The effect of pier size on the temporal variation of local scour

Both the time to reach the equilibrium scour depth and the equilibrium scour depth increase with the pier diameter. Melville and Coleman (2000) stated that, for a narrow pier in which the ratio of the pier diameter to the flow depth, b/h, is smaller than 0.7, the scour depth only depends on the pier diameter. Figure 4.9 shows that the relative scour depth, d_s/b, increased with dimensionless time and it is larger for smaller relative pier diameter. This finding is not in contradiction with the increase of the scour depth with the pier diameter since it refers to non-dimensional values.
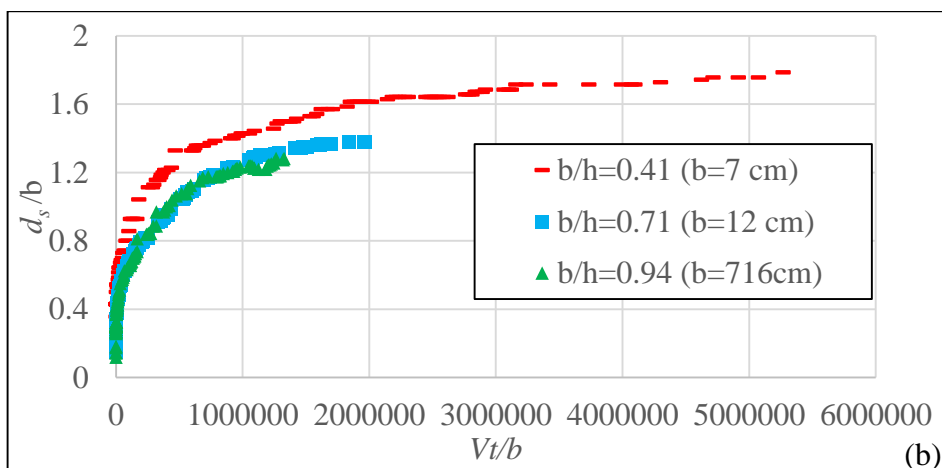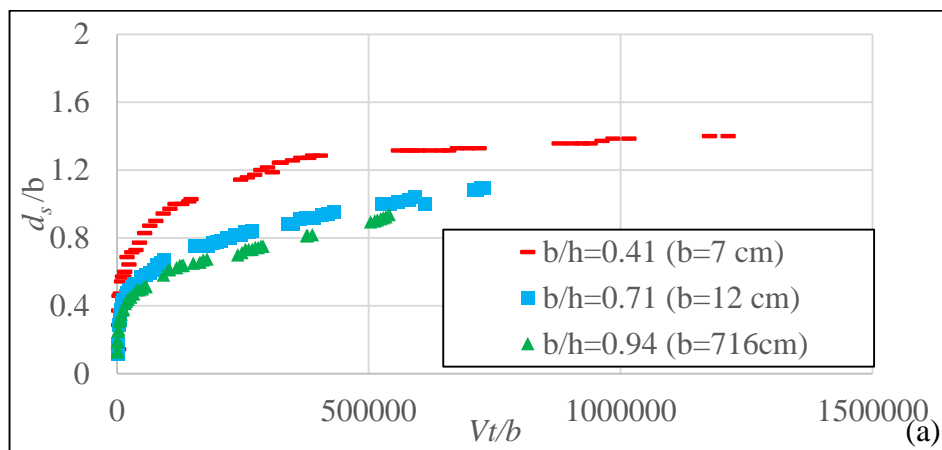
Figure 4.9 The relative scour depth d_s/b increased with dimensionless time (a) channel width 177 cm, (b) channel width 120 cm, (c) channel width 74 cm.

4.1.3 The effect of channel width on temporal variation of local scour
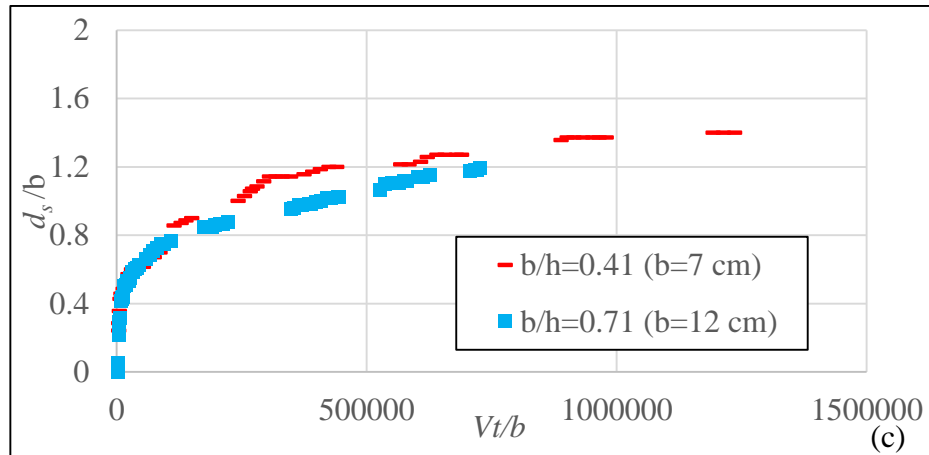
In this study, the experiments were carried out for three different channel widths, with the purpose of revisiting the effect of the channel width on the local scour depth. This effect can be important for comparatively narrow channels.

Whenever a pier is inserted within the flow, the flow accelerates around the pier due to the reduction of the cross-section area and the flow structures mentioned in Section 2.4.4 lead to scouring. For wide channels, the conveyance of the scour hole at equilibrium compensates the conveyance suppressed by the pier in such a way that, sidewise, a few pier widths away from the pier, the flow field remains undisturbed (as if there were no pier). For narrow channels, if the scour holes could be the same for wide channels, they would not guarantee the necessary conveyance unless the velocity could increase in relative terms. Increased velocities imply increased bed shear and further scouring. For this reason, the scour hole in narrow channels must be deeper to guarantee the required conveyance for velocities compatible with the condition of the beginning of motion. This increment of the scour depth is usually called contraction scour.

From above, the question of what is a narrow channel arises. Cunha (1973) and Franzetti et al. (1994) stated that, for $b/B < 0.09 – 0.10$ [32-45], the contraction effect is negligible, meaning that the contribution of contraction to the scour depth is null or practically null. In most experimental studies, the ratio of the pier diameter to the

49

channel width, *b/B*, is kept as small as possible (typically *b/B* < 0.1) to avoid contraction and wall effects on local scouring around the bridge piers.

Ballio (2000) conducted several long duration experiments (1.5 to 6 weeks) around bridge abutments under the clear-water conditions and found that for *b/B* < 0.33 the blockage ratio does not significantly affect the time evolution of the phenomenon [55].

Figures 4.10 to 4.12 show the evolution of the non-dimensional maximum local scour depth, *ds/b,* with the non-dimensional time, *Vt/b*, for the pier diameters, *b*, equal to 7 cm, 12 cm and 16 cm, respectively. It is clear that the effect of contraction on the scour process is not present in the case of *b* = 7 cm (Figure 4.10). The same seems to be true for *b* = 12 cm (Figure 4.11), although there may be a smaller scour rate in experiment A12w, meaning that there may be a small contraction effect in experiments A12 and A12n. Contraction scouring is more evident in the experiments for *b* = 16 cm (Figure 4.12).
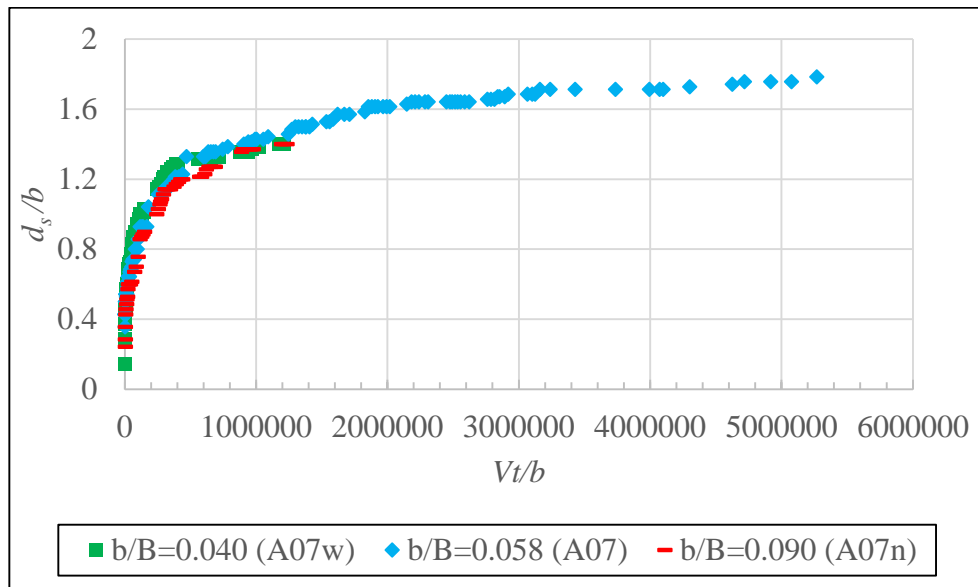
Figure 4.10 Dimensionless temporal development of the maximum local scour depth.
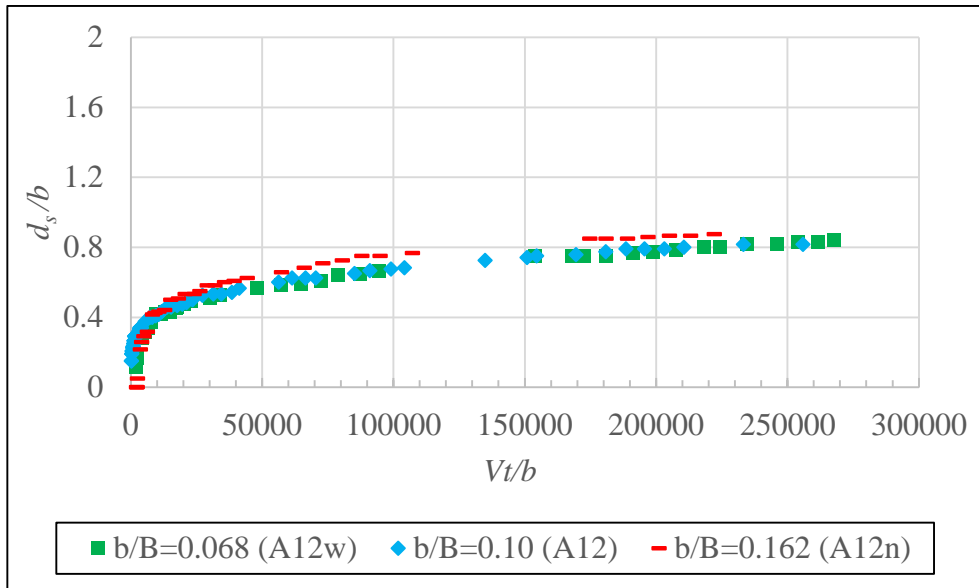
Figure 4.11 Dimensionless temporal development of the maximum local scour depth.
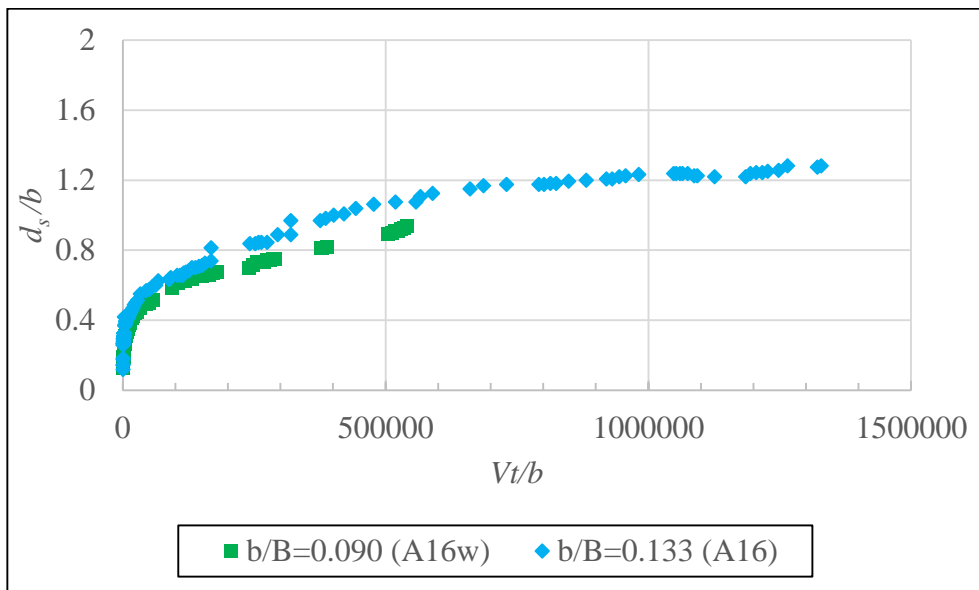
Figure 4.12 Dimensionless temporal development of the maximum local scour depth.

4.2 Equilibrium Local Scour Depth

4.2.1 Comparison of experimental result with the predictors given for local scour depth

The maximum, equilibrium, final or end scour depths were calculated according to the equations given in Chapter 2. The results are presented in Table 4.5 and Figure 4.13.

Table 4.4 Scour depth calculated by the predictors presented in Chapter 2 (in cm).

EXP	A07w	A12w	A16w	A07	A12	A16	A07n	A12n
Laursen (1958) (d_{sm})	14.6	19.1	22.1	14.5	19.1	22.1	14.6	19.1
Hancu (1971) (d_{sf})	7.9	11.3	13.7	7.6	10.9	13.2	7.6	10.9
Breuers (1977) (d_{sm})	3.4	5.3	6.2	2.5	3.8	4.5	2.5	3.9
Jain and Fischer (1979) (d_{sm})	12.7	18.6	22.7	12.7	18.6	22.7	12.7	18.6
Citale (1981) (d_{se})	17.5	30.0	40.0	17.5	30.0	40.0	17.5	30.0
CSU Equation (1988) (d_{se})	10.6	15.1	18.2	10.4	14.7	17.7	10.4	14.7
Johnson (1992) (d_{se})	10.0	16.9	22.4	9.8	16.7	22.1	9.8	16.7
Goa (1993) (d_{se})	2.6	3.9	4.9	1.8	2.8	3.6	1.8	2.9
Melville (1997) (d_{se})	10.5	17.8	20.6	9.9	16.9	19.5	9.9	16.9
May (2002) (d_{se})	6.3	4.5	8.7	5.4	6.7	7.5	5.4	6.7
Lança et al. (2013) (d_{se})	18.2	29.6	32.2	18.2	29.6	32.2	18.2	29.6
Aksoy and Eski (2016) (d_{sm})	7.7	11.6	14.5	7.4	11.1	13.9	7.4	11.0
$d_{s,ed}$	9.8	13.1	15.0	12.5	16.5	20.5	9.8	14.8

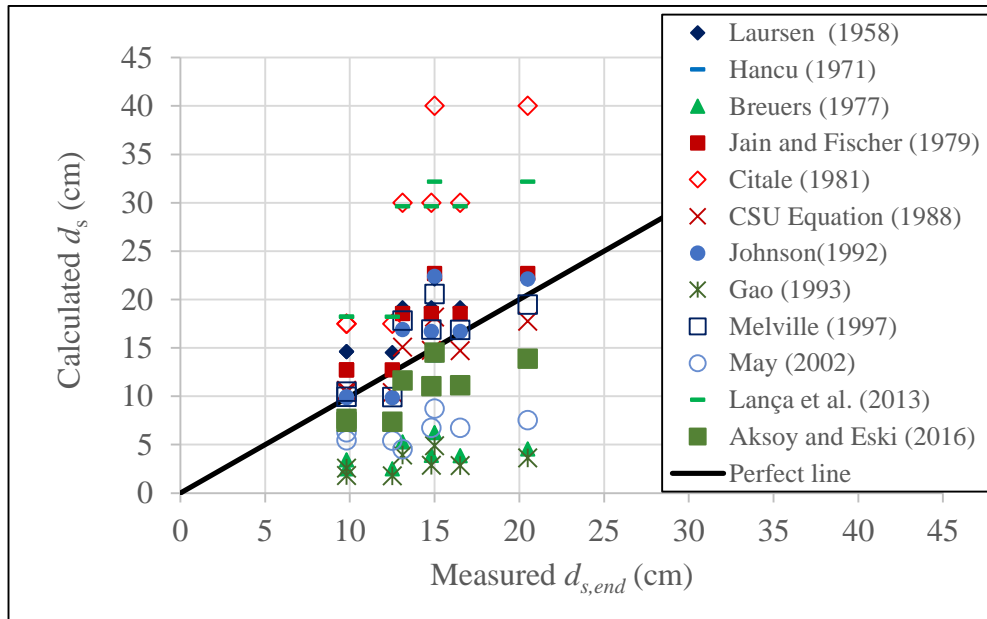**Figure 4.13** Calculated scour depth by using the predictors (section 2.5) with measured end scour depth.

Assuming that the end scour depths measured in the present study are sufficiently close to the equilibrium value – since the experiments lasted until approximately 4 days – Figure 4.13 indicates that the predictors of Gao (1993), May (2002) and Aksoy and Eski (2016) clearly underestimate the scour depth. This result should not be ignored in engineering practice as the use of these predictors may have very negative consequences. On the other hand, the predictors of Citale (1981) and Lança et al. (2013) seem to largely over-predict the scour depth, which may be partly explained by the fact that $d_{s, end}$ where not really the equilibrium values.

4.2.2 Analysis of local scour considering time to equilibrium criteria

According to the analysis presented in chapter 4.1, it is not possible to conclude that equilibrium scour depth was reached for any of the experiments, suggesting the asymptotic character of the scouring process. Still, according to section 2.4.6, some authors define either the time to equilibrium or the time required to stop experiments, particularly for clear-water flow conditions. Next, some of these contributions are assessed based on the experimental results.

Melville and Chiew (1999) stated that equilibrium is reached when the scour rate in 24 hours reduces to 5% of the pier diameter. Franzetti et al. (1994) suggested the predictor to calculate the time to equilibrium presented in section 2.4.6. Coleman et al.

(2003) defined the equilibrium time as the time at which the rate of the scour reduces to 5% of the smaller of the pier diameter or the flow depth in a 24 hour period. Grimaldi (2005) suggested a more restrictive criterion, namely, the reduction of scour rate to less than 0.05b/3 in a 24 hour period. Figure 4.14 shows the temporal variation of scour rate, $\Delta d_s/24hr$ for the experiment A16w. The equivalent figures for the other experiments are presented in Appendix II.
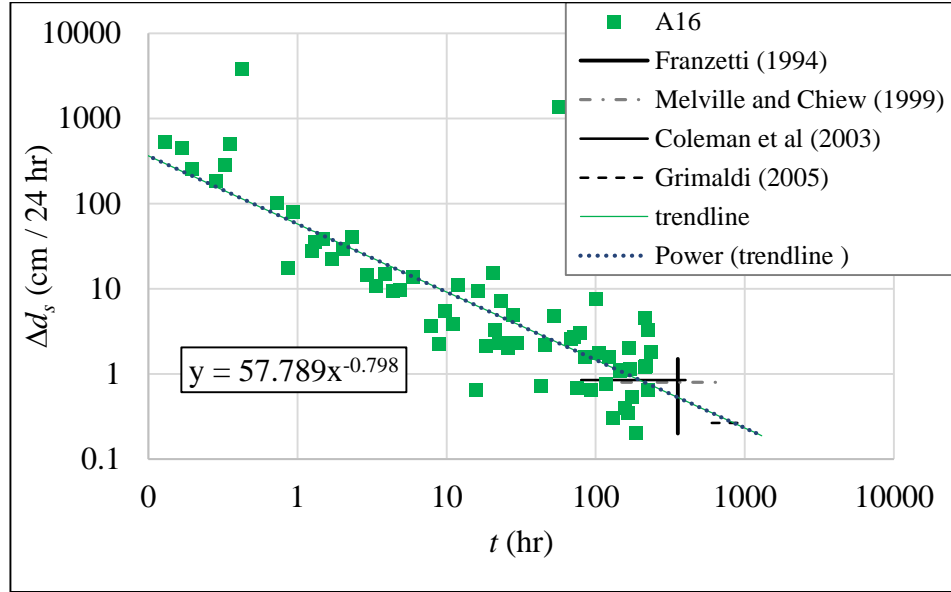
Figure 4.14 The temporal variation of scour rate, $\Delta d_s/24hr$, with respect to time.

Equation 4.3 is a power trend line fitted to the data

$$\frac{\Delta d_S}{24\ hr} = 57.789\ t^{-0.798} \qquad (4.3)$$

The criterion of Franzetti et al. (1994) is shown as a vertical line passing through the curve of the scour rate at $t = 337$ hr. The corresponding $\Delta d_s/24hr$ was calculated on the adjusted line as 0.48 cm/24 hr. The contributions of Melville and Chiew (1999), Coleman et al. (2003) and Grimaldi (2005) led to values of $\Delta d_s/24hr$ equal to 0.80 cm, 0.85 cm and 0.27 cm, as illustrated by horizontal lines corresponding to time equal to 179 hr, 165.1 hr and 773.1 hr, respectively. Therefore, the scour depth value at those times needs to be obtained by extrapolating the scour data. For this purpose, the first 24 hour data is excluded not to dominate in calculations. Figure 4.15 shows the fitted curve for experiment A16w.
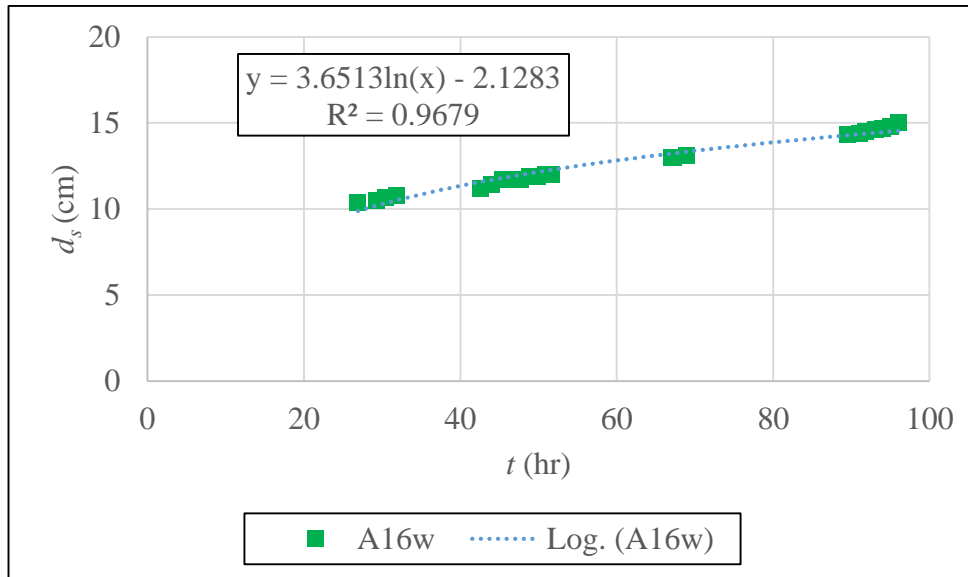
Figure 4.15 Show the fitted equation and its graph for the experiment A16w.

Table 4.5 shows the summary of the scour rate per 24 hr, ($\Delta d_s/24$ hr), corresponding equilibrium time, t_e, in hr and the calculated equilibrium scour depths, $d_{se,c}$ in cm. It is to be noticed here that the longer is the equilibrium time, the larger is the calculated scour depth. Figure 4.16 show the calculated scour depth by using the predictors (section 2.5) with measured end scour depth.

Table 4.5 Comparison of equilibrium time, t_e, in hr and $\frac{\Delta d_s}{24\,hr}$, $d_{se,c}$ and $d_{s,end}$ in cm.

| EXP	ABR	Franzetti et al. (1994) $\frac{Vt}{b} > 2x10^6$	Melville and Chiew (1999) $\Delta d_s < 0.5b$	Coleman et al. (2003) $\Delta d_s < 0.5h$	Grimaldi (2005) $\Delta d_s < 0.5b/3$	Experimental values	
A07w	$\frac{\Delta d_s}{24hr}$	N.A*	0.4	0.9	0.1	t_{dur}	$d_{s,end}$
	t_e	148.0	136.8	56.3	410.7	94.4	9.8
	$d_{se,c}$	10.2	10.1	9.4	11.0		
A12w	$\frac{\Delta d_s}{24hr}$	N.A*	0.6	0.9	0.2	t_{dur}	$d_{s,end}$
	t_e	253.0	181.5	118.7	691.7	97.23	13.1
	$d_{se,c}$	15.6	14.7	13.5	18.5		
A16w	$\frac{\Delta d_s}{24hr}$	N.A*	0.8	0.9	0.3	t_{dur}	$d_{s,end}$
	t_e	337.0	179.0	165.1	773.1	96.02	15.0
	$d_{se,c}$	19.1	16.8	16.5	22.2		
A07	$\frac{\Delta d_s}{24hr}$	N.A*	0.4	0.9	0.1	t_{dur}	$d_{s,end}$
	t_e	156.0	482.8	142.0	2197.0	410	12.5
	$d_{se,c}$	11.1	12.9	10.9	15.3		
A12	$\frac{\Delta d_s}{24hr}$	N.A*	0.6	0.9	0.2	t_{dur}	$d_{s,end}$
	t_e	267.0	220.9	145.5	841.9	262	16.5
	$d_{se,c}$	17.2	16.6	15.1	21.1		
A16	$\frac{\Delta d_s}{24hr}$	N.A*	0.8	0.9	0.3	t_{dur}	$d_{s,end}$
	t_e	356.0	154.4	142.0	984.5	237	20.5
	$d_{se,c}$	22.4	18.8	18.5	26.7		
A07n	$\frac{\Delta d_s}{24hr}$	N.A*	0.4	0.9	0.1	t_{dur}	$d_{s,end}$
	t_e	155	229.1	80.7	834.5	96.07	9.8
	$d_{se,c}$	10.6	11.2	9.6	13.1		
A12n	$\frac{\Delta d_s}{24hr}$	N.A*	0.6	0.9	0.2	t_{dur}	$d_{s,end}$
	t_e	267.0	202.9	133.4	834,5	96.9	14.3
	$d_{se,c}$	17.1	15.2	15.0	20.3		

*: Not Applicable
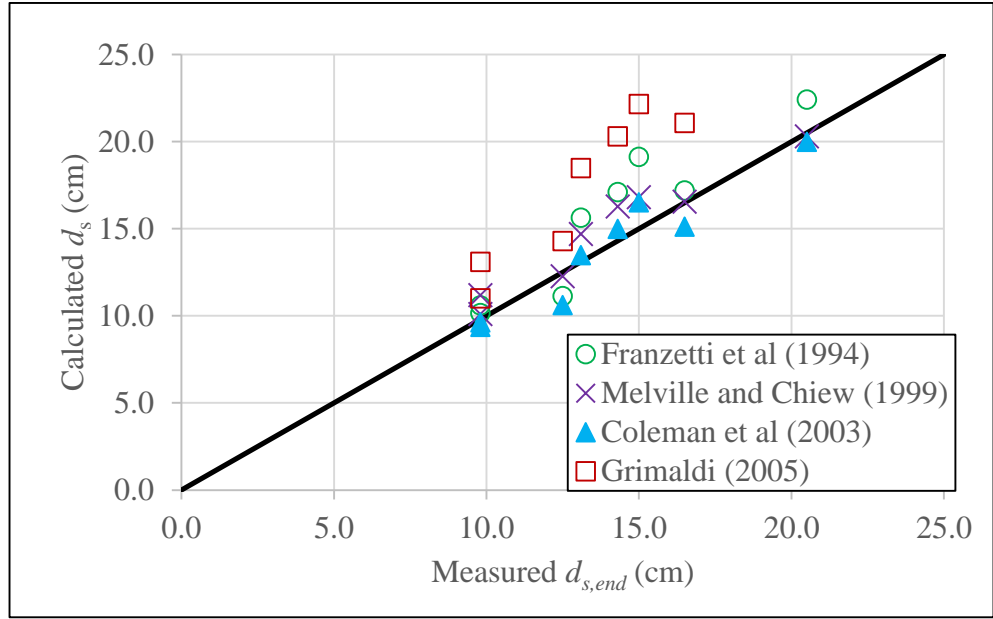
Figure 4.16 Calculated scour depth by using the predictors (section 2.6) with measured end scour depth.

4.2.3 Analysis of local scour by fitting the B_4 polynomial to the data

Besides those contributions discussed in the previous section, some don't even consider the existence of equilibrium time, assuming that equilibrium scour depth is reach at infinite time. Among these, Bertoldi and Jones (1998) suggested the fitting of a 4 parameter polynomial to scour depth data measured for a short time (days) to get the equilibrium scour depth []. Their polynomial reads

$$B_4(t) = \ell_1 \frac{t/\tau_1}{1 + t/\tau_1} + \ell_2 \frac{t/\tau_2}{1 + t/\tau_2} \qquad (4.4)$$

where ℓ_1, ℓ_2 (length) and τ_1, τ_2 (times) can be obtained from the scour depth registered along that short time. The summation of $\ell_1 + \ell_2$ gives the equilibrium scour depth as indicated in Table 4.6, where the values of RMSE, MAE and R^2 resulting from the adjustment procedure are also included.

Table 4.6 Equilibrium scour depth by B_4 polynomial in (cm).

EXP	A07w	A12w	A16w	A07	A12	A16	A07n	A12n
$d_{se}=\ell_1+\ell_2$	10.5	18.8	20.6	11.4	19.6	23.9	11.2	32.4
RMSE	3.09	1.79	3.94	14.04	3.16	3.49	2.91	2.63
MAE	1.91	1.28	3.12	11.06	2.40	2.73	2.34	1.64
R^2	0.991	0.998	0.992	0.899	0.996	0.996	0.993	0.995
$d_{s,end}$	9.8	13.1	15.0	12.5	16.5	20.5	9.8	14.8

It is observed that the longer is the equilibrium time, the higher scour depth occurred, taking into consideration the criteria of Melville and Chiew (1999) is suitable for the experiments with 16 cm pier diameter and Coleman et al. (2003) for the rest of the experiments.

Figure 4.17 compares the calculated scour depth by using the B_4 polynomial with the measured end scour depth. The end measured scour depth and the calculated equilibrium scour depth by B_4 function were close to each other for smaller pier diameter ($b = 7$ cm).
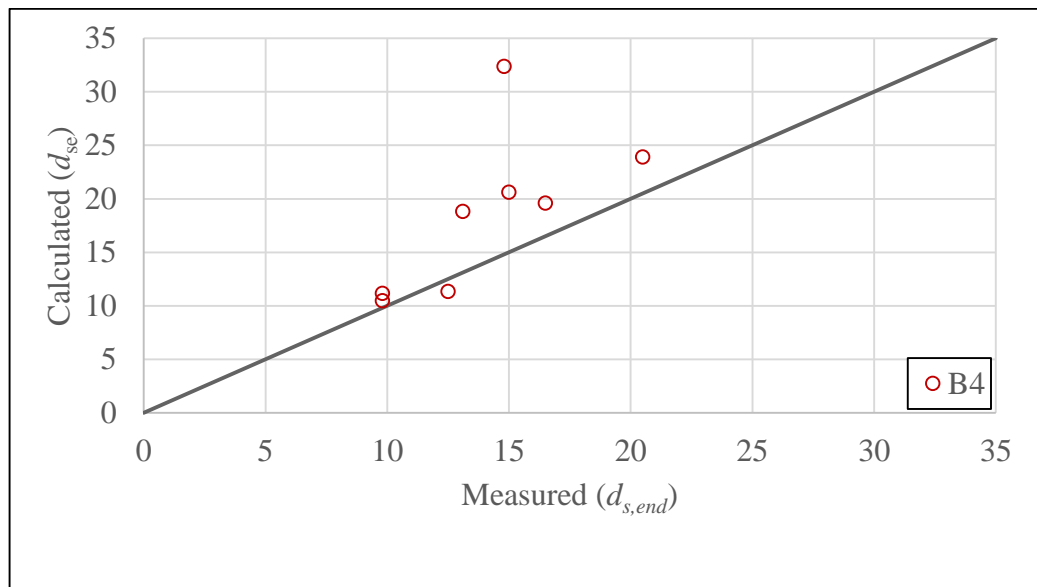

Figure 4.17 Calculated scour depth by using the B_4 polynomial with measured end scour depth.

4.2.4 The Effect of Pier Size and Channel Width on the Equilibrium Scour Depth

As discussed in chapter 4.1.3, the width of the channel as well as the pier size influence the equilibrium scour depth as they influence the temporal evolution of the scour depth. Here, this effect is discussed quantitatively by considering the values of some non-dimensional parameters, as given in Table 4.7. This table also shows the non-dimensional equilibrium scour depths at the "equilibrium times" given by Franzetti et al. (1994), Melville and Chiew (1999), Coleman et al. (2003), Grimaldi (2005) as calculated on the adjusted logarithmic curves described in 4.2.2 (see Figure 4.14). Finally, the table includes the equilibrium scour depths issued through the adjustment of the B_4 polynomial of Bertoldi and Jones (1998).

Table 4.7 Scour depths calculated for the "equilibrium times" of Franzetti et al. (1994), Melville and Chiew (1999), Coleman et al. (2003), Grimaldi (2005) and Bertoldi and Jones (1998).

	d_{se}/b	A07w	A12w	A16w	A07	A12	A16	A07n	A12n
	b/B	0.040	0.068	0.090	0.058	0.100	0.133	0.095	0.162
	h/b	2.43	1.42	1.06	2.43	1.42	1.06	2.43	1.42
See section 4.2.2	Franzetti et al. (1994)	1.45	1.30	1.20	1.59	1.43	1.40	1.51	1.42
	Melville and Chiew (1999)	1.44	1.22	1.05	1.75	1.38	1.27	1.60	1.36
	Coleman et al. (2003)	1.34	1.12	1.03	1.52	1.26	1.25	1.38	1.25
	Grimaldi (2005)	1.57	1.54	1.38	2.04	1.76	1.63	1.87	1.69
See section 4.2.3	B_4	1.50	1.57	1.29	1.62	1.63	1.49	1.59	2.70
	$d_{se,end}/b$	1.40	1.09	0.94	1.79	1.38	1.28	1.40	1.19

The effect of the contraction ratio b/B can be better investigated by plotting the calculated equilibrium values of dimensionless scour depth against the contraction ratio b/B. The scour depth generally increases with the contraction ratio, as shown in Figure 4.18 and Figure 4.19. In Figure 4.18, the equilibrium scour was determined at the time to equilibrium given by Melville and Chiew (1999). Figure 4.19, refers to the equilibrium scour at infinite time obtained by adjusting the polynomial B_4 to the measurements. The rest of figures can be found in Appendix III.
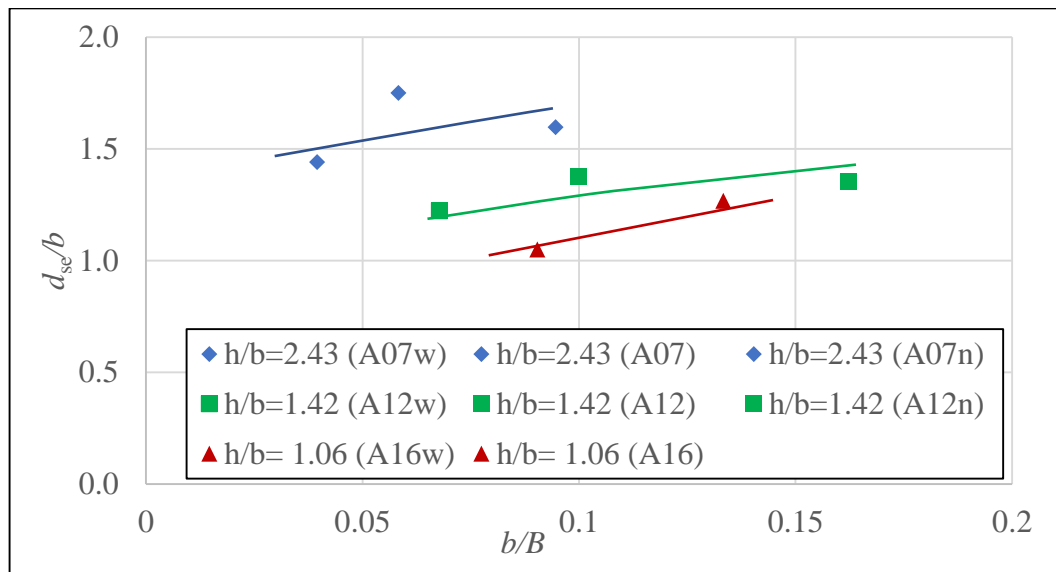

Figure 4.18 The equilibrium dimensionless scour depth with constriction ratio by Melville and Chiew (1999).
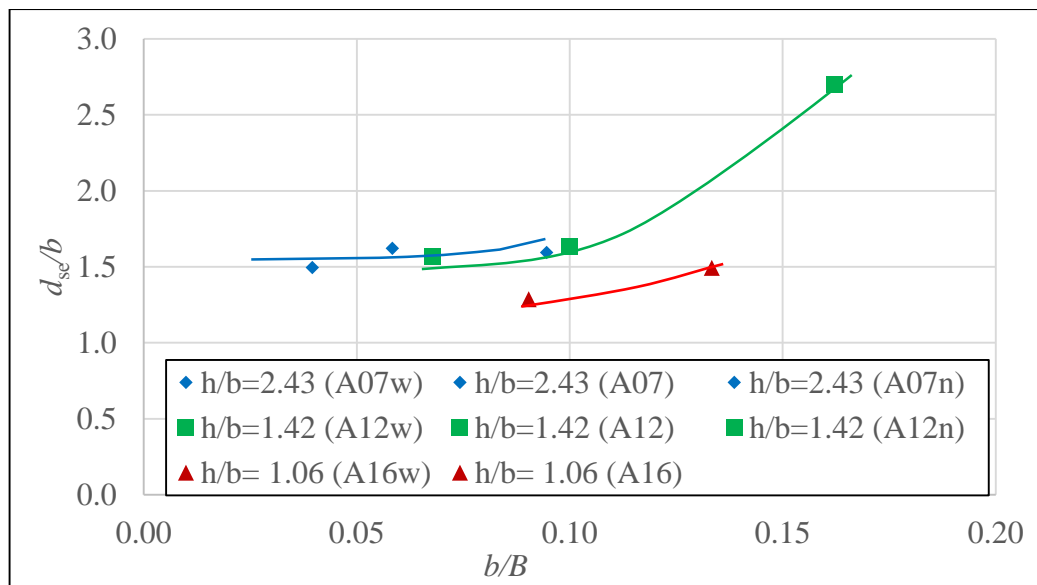

Figure 4.19 The equilibrium dimensionless scour depth with constriction ratio by (B_4).

It is observed that the channel width does not influence scouring for small pier diameters whereas it does increase the scour depth for wider (relative) diameters.

According to section 2.3, equation (2.5c), least squares regression analysis in the form

$$\frac{d_{se}}{b} = c_1 \left(\frac{h}{b}\right)^{c_2} \left(\frac{b}{B}\right)^{c_3} \tag{4.4}$$

was performed. The constants c_1 and the powers c_2 and c_3 obtained are given in Table 4.8. The RMSE, MAE and R^2 values are also given in the same Table. The figures are given in Appendix IV.

Table 4.8 Constants c_1, c_2 and c_3 of equation (4.4) and the RMSE, MAE and R^2 values.

		c1	c2	c3	RMSE	MAE	R2
See section 4.2.2	Franzetti et al. (1994)	1.56	0,25	0.0891	4.12	4.12	0.7376
	Melville and Chiew (1999)	1.47	0.47	0.1199	6.23	5.59	0.8225
	Coleman et al. (2003)	1.32	0.33	0.0804	5.81	5.13	0.7207
	Grimaldi (2005)	2.08	0.34	0.1524	6.88	5.95	0.6350
See section 4.2.3	B_4	5.18	0.36	0.5364	16.76	14.49	0.5112
	$d_{se,end}/b$	1.20	0.44	0.0537	11.94	11.16	0.5642

5. CONCLUSION

Local scour that occurs around bridge piers is the main reason for their failure. Thus, to predict the scour depth around piers and take necessary precautions is essential in Civil Engineering. Several factors affect the scour depth, such as, for instance, the approach flow depth, flow intensity, pier diameter or width or the sediment characteristics. Among these factors, the present study intends to investigate the effect of channel width and flow contraction on the temporal evolution and the equilibrium scour depth.

An experimental study was conducted in a 15 m long and 0.90 m high rectangular flume with a horizontal bed made of uniform sand having a median diameter of 1.04 mm, by imposing three different pier diameters, namely, 7 cm, 12 cm and 16 cm. The channel widths tested were 74 cm, 120 cm and 177 cm and the duration of the experiments was selected to be at least approximately 4 days. The flow depth and flow intensity were kept constant for all the experiments as 17 cm and 0.6, respectively.

During the experiments, the maximum scour depth was observed on the pier sides in the initial stages of the scouring process and then shifted to the upstream face of the pier where the horseshoe vortex develops. The time evolution for all experiments was analyzed and the experimental results were compared with the predictors given in the literature and summarized in Chapter 2 for the evolution of local scour. It was revealed statistically that, in average, the time evolution predictors proposed by Franzetti et al. (1982) and Oliveto and Hager (2002) were in accordance with the experimental results. The effect of pier size on the temporal variation of local scour and the effect of channel width on temporal variation of local scour were also discussed. It was confirmed that contraction scouring was more evident in the experiments with the wider diameter.

In the literature various predictors were proposed by researchers to calculate maximum, equilibrium and final or end scour depths. When compared with the experimentally obtained end depths, it is observed that Laursen (1958), Jain and Fischer (1979), Citale (1981) and Lança et al. (2013) predicted scour depths higher than the end scour depths whereas Gao (1993), Breusers (1977) and May (2002) predicted lower scour depths.

As declared in Chapter 4, it is not possible to conclude that equilibrium scour depth was reached for any of the experiments, suggesting the asymptotic character of the scouring process. Still, some authors define either the time to equilibrium or the time required to stop experiments. Local scouring was analyzed at the times given by those authors. It is observed that, except for Grimaldi (2005), the scour depths corresponding the equilibrium times calculated by the mentioned methods are in accordance with the end scour depth values of the performed experiments. The apparent over-prediction associated with Grimaldi's proposal reflects the simple fact that the time suggested by this author is much longer than those of the other predictors.

Some researchers do not consider the existence equilibrium time, assuming that equilibrium scour depth is reach in infinite time. Bertoldi and Jones (1998) suggested the fitting of a 4 parameter polynomial to the scour depth data to get the equilibrium scour depth. It is revealed that the calculated scour depth by using the B_4 polynomial are slightly greater than those measured as the end scour depth.

The effect of pier size and channel width on local scour was analyzed after performing a dimensional analysis and deriving a generic equation with three dimensionless parameters (see Equation 2.5c).

The variation of the equilibrium values of dimensionless scour depth with the contraction ratio, b/B, was plotted by grouping the experiments in three categories of h/b, namely 2.43, 1.42 and 1.06, and the corresponding curves were obtained. It is illustrated that d_{se}/b increases with h/b whereas changes in b/B have almost no appreciable effect since all curves are almost horizontal (see Figure 4.18, Figure 4.19). To clarify this result quantitatively regression analysis was performed to obtain the constant c_1 and power values c_2 and c_3 proposed in equation (4.4) that are also listed in Table 4.8. As can be seen in this Table, the small values of c_3 with respect to c_2, proves that the effect of b/B on d_{se}/b is negligible for the experimental scenarios conducted in this study. Also, for the equilibrium scour depth values obtained by fitting the B_4 polynomials it is illustrated that neglecting the effect of b/B would be acceptable for values of $b/B \approx 0.15$.

One may conclude that as long as the contraction ratio b/B is smaller than 0.10, the dimensionless channel width doesn't have a significant effect on local scour depth,

which is in accord with Cunha (1973), Franzetti et al. (1994) and Ballio (2000). It should be noted that, further experimental data are needed to verify the present conclusion due to the limitations of the present study.

REFERENCES

1. Wardhana K and Hadipriano F. Analysis of Recent Bridge Failures in the United States: Journal of Performance of Constructed Facilities; 2003.

2. Tuna T. Köprü Çökme Noktasında. Retrieved, from haberhurriyeti: http://www.haberhurriyeti.com/kopru-cokme-noktasinda. 159293.html; 2016.

3. Yanmaz A and Caner A. Çaycuma Köprüsünün Çökmesi Üzerine Görüşler: Türkiye Köprü ve İnşaat Cemiyeti; Ankara 2012.

4. Yanmaz M A. Reliability Simulation of Scouring Downstream of Outlet Facilities: Turkish J. Eng. Env. Sci. 27 (2003), 65 – 71; 2002.

5. Sondevir. Köprü Bir Kez Daha Çöktü, Retrieved from Son Devir Ekonomi: http://ekonomi.dunyabulteni.net/gundem/65171/kopru-bir-kezdaha coktu; 2012.

6. Lagasse P F and Richardson E V. compendium of stream stability and bridge scour papers: Journal of Hydraulic Engineering; ASCE 127(7), 531 533; 2001.

7. Dey S. Local scour at piers, part 1. A review of development of research: International Journal of Sediment Research, IJSH, 1997; 12(2): 23-46.

8. Kılınc B .Experimental investigation of local scouring around bridge piers under clear-water conditions: M.Sc. Thesis, Izmir Kâtip Çelebi University. Turkey; 2019.

9. Richardson E V and Davis S R. Evaluating Scour at Bridges: Hydraulic Engineering Circular (18), Federal Highway Administration; 1995.

10. Cheremisinoff P N, Cheremisinoff N P and Cheng S L. Hydraulic mechanics 2. Civil Engineering Practice: Technomic Publishing Company, Inc., Lancaster, Pennsylvania, U.S.A. 780 p; 1987.

11. Ettema R E. Scour at bridge piers: Rep. No. 236, School of Engrg. The Univ. of Auckland, New Zealand; 1980.

12. Breussers H N C and Raudkivi A J. Hydraulic Structures Design Mannual-Hydraulic Design Considerations. Chapter-5, Scour at Bridge Piers: Balkama Publications, Rotterdam, the Netherlands; 1991.

13. Raudkivi A J. Loose boundary hydraulics. Balkema, Rotterdam, 4. Edition; 1998.

14. Alabi P D. Time development of local scour at a bridge pier fitted with a collar: M.Sc. Thesis, University of Saskatchewan, Canada; 2006.

15. Breusers H N C, Nicollet G and Shen H W . Local scour around cylindrical piers: J. Hydr. Res, 1977; 15(3), 211-252

16. García M H editor. Sedimentation engineering: Processes, measurements, modeling, and practice, volume 110 of ASCE manuals and reports on engineering practice. American Society of Civil Engineers, Reston and Va; 2008.

17. Neill C R. Local scour around piers: Journal of Hydraulic Research, 1978; 16(3):259–262.

18. Müller D S and Wagner C R. Field observations and evaluations of streambed scour at bridges: Federal Highway Administration; 2005.

19. Fael C, Lança R, Cardoso A H. Effect of pier shape and pier alignment on the equilibrium scour depth at single piers: International Journal of Sediment Research, 2016; 31(3): 244–250 https://doi.org/10.1016/j.ijsrc.2016.04.001

20. Laursen E and Toch A. Scour around bridge piers and abutments: Iowa Highway Research Board Bulletin (4); 1956.

21. Melville B W and Sutherland A I. Design method for local scour at bridge piers: J. Hydr. Engrg, ASCE, 1988; 114(10), 1210-1226.

22. Melville B W and Coleman S E. Bridge scour: Water Resources, Fort Collins, Colo 2000.

23. Dietz J W. Systematische Modellversuche über die Pfeilerkolkbildung. Mitteilungsblattder Bundesanstalt für Wasserbau (31), Karlsruhe; 1972.

24. Link O. Time Scale of Scour around a Cylindrical Pier in Sand and Gravel: Third Chinese-German Joint Symposium on Coastal and Ocean Engineering National Cheng Kung University, Tainan November 8-16, 2006

25. Chabert J and Engeldinger P. Etude des affouillements autour des piles des ponts: Laboratoire d'Hydraulique, Chatou, France (in French); 1956.

26. Shen H W, Schneider V R and Karaki S. Local scour around bridge piers: Journal of the Hydraulics Division, 1969; 95(HY 6):1919–1940.

27. Chiew Y M . Local scour at bridge piers: Rep. No. 355, School of Engineering, Univ. of Auckland, Auckland, New Zealand; 1984.

28. Raudkivi A J and Ettema R. Clear water scour at cylindrical piers: Journal of Hydraulic Engineering, ASCE, 1983; 109(HY3), 338-350.

29. Franzeti S, Larcan E and Mignosa P. Influence of tests duration on the evaluation of ultimate scour around circular piers: Proc., Int. Conf. on the Hydr. Modelling of Civ. Engrg. Struct, BHRA Fluid Engineering, Cranfield, Bedford MK43 OAJ, England, 1982; 381–396

30. Cardoso A H and Bettess R. Effects of time and channel geometry on scour at bridge abutments: J. Hydr. Engrg. ASCE, 1999; 125(4): 388-399.

31. Melville B W and Chiew YM. Time scale for local scour at bridge piers: J. Hydraul. Eng. 1999; 125~1. 59–65.

32. Franzetti S, Malavasi S, Piccinin C . Sull'Erosione alla Base delle Pile Di Ponte in Acque Chiare: XXIV Convegno di Idraulica e Costruzioni Idrauliche. Napoli, p. 1994; 1-13

33. Coleman S E, Melville B W and Gore L. Fluvial Entrainment of Protruding Fractured Rock: J. of Hydr. Engg. ASCE. 2003; 129(11), pp. 872-884

34. Mia F and Nago H. Design method of time-dependent local scour at circular bridge pier: Journal of Hydraulic Engineering. 2003; 129(6):420–427.

35. Oliveto G, and Hager W H. Temporal evolution of clear-water pier and abutment scour: J. Hydraul. Eng, 2002; 128(9), 811–820.

36. Grimaldi C. Non-conventional countermeasures against local scouring at bridge piers: Ph.D. thesis, Hydraulic Engineering for Environment and Territory, Univ. of Calabria, Cosenza, Italy; 2005.

37. Fael C M S, Simarro G, Martin-Vide J P and Cardoso A H. Local scour at vertical-wall abutments under clear water flow conditions: Water Resour. Res. 2006; 42(10), W10408.

38. Setia B. Equilibrium scour depth time: 3rd IASME/WSEAS International Conference on Water Resources, Hydraulics and Hydrology (WHH '08), University of Cambridge, UK. 2008; 114–117.

39. Sheppard D M. An overlooked local sediment scour mechanism: Transportation Research Record. 1890, Transportation Research Board, Washington, D.C. 2004; 107–111.

40. Lee S O and Sturm T W. Effect of sediment size scaling on physical modeling of bridge pier scour: Journal of Hydraulic Engineering, 2009; 135(10):793–802.

41. Laursen E M. The Total Sediment Load of Streams: Journal of the Hydraulics Division, ASCE, No. HY1; 1958.

42. Hancu S. Sur le calcul des affouillements locaux dams la zone des piles des ponts: Proc, 14th IAHR Congress, Vol. 3, International Association for Hydraulic Research, Delft, the Netherlands. 1971; 299–313.

43. Jain S C and Fischer E E. Scour around circular bridge piers at high Froude numbers: Rep. No. FHWA-RD-79-104. FHWA, Washington, D.C; 1979.

44. Citale S V. Shape and Mobility of River Meanders: Proc. XIX Congress of IAHR, Volume 2, New Delhi P. 1981; 281-286.

45 Cunha LV. discussion, Journal of Hydraulics Division: 1973; 98(HY9), pp. 1637-1639.

46. Johnson P A. Reliability-based pier scour engineering: Journal of Hydraulic Engineering. 1992; 118(10):1344–1358.

47. Richardson J R and Richardson E V. Bridge scour evaluation: García M H, editor, Sedimentation engineering, volume 110 of ASCE manuals and reports on engineering practice, pages 505–542. American Society of Civil Engineers, Reston and VA; 2008.

48. Gao D, Posada L and Nordin C F. Pier scour equation used in china: Richardson E V and Lagasse P F, editors, Stream stability and scour at highway bridges, pages 217–222. The Society, Reston and Va; 1999.

49. Melville B W. Pier and abutment scour—an integrated approach: J. Hydr. Engrg. ASCE. 1997; 123(2), 125–136.

50. Lança RM, Fael CS, Maia RJ, Peˆgo JP, Cardoso A H. Clear-water scour at comparatively large cylindrical piers: J Hydraul Eng (ASCE). 2013; 139(11):1117–1125.

51. Aksoy A O, Eski O Y. Experimental investigation of local scour around circular bridge piers under steady state flow conditions: Journal of the South African Institution of Civil Engineering. J. S. Afr. Inst. Civ. Eng. 2016; 58(3), 21–27.

52. Sumer B M, Christiansen N, Fredsoe J. Time scale of scour around a vertical pile: Second international offshore and polar engineering conference. International Society of Offshore and Polar Engineers. 1992.

53. Kothyari U C, Hager W H and Oliveto G. Generalized approach for clear-water scour at bridge foundation elements: J. Hydraul. Eng. 2007; 133(11), 1229–1239.

54. Aksoy A O, Bombar G, Arkış T, Güney MS. Study of the time dependent clear-water scour around circular bridge piers: J Hydrol Hydromech. 2017; 65(1):26–34.

55. Ballio F. Local and Contraction Scour at Bridge Abutments: Water Resources. 2000

56. Simarro G, Cristina M S, Fael C and Cardoso A H: Estimating Equilibrium Scour Depth at Cylindrical Piers in Experimental Studies: 2011; (ASCE) HY.1943-7900.0000410.
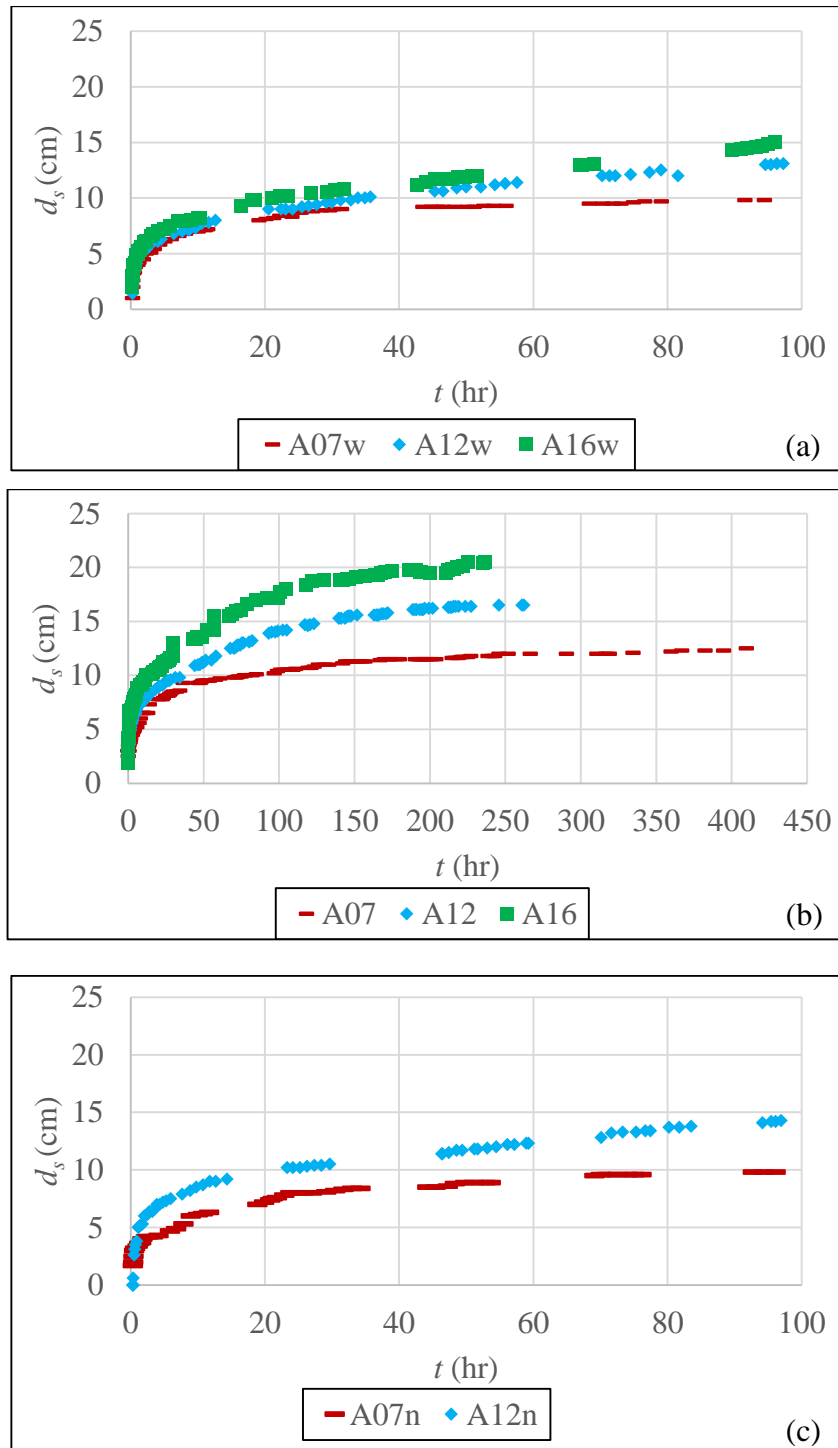
APPENDIX I

TEMPORAL EVOLUTION OF LOCAL SCOUR DEPTH

Figure A1.1 Temporal evolution of local scour depth in front of the pier (a) channel width 177 cm, (b) channel width 120 cm, (c) channel width 74 cm.

APPENDIX II

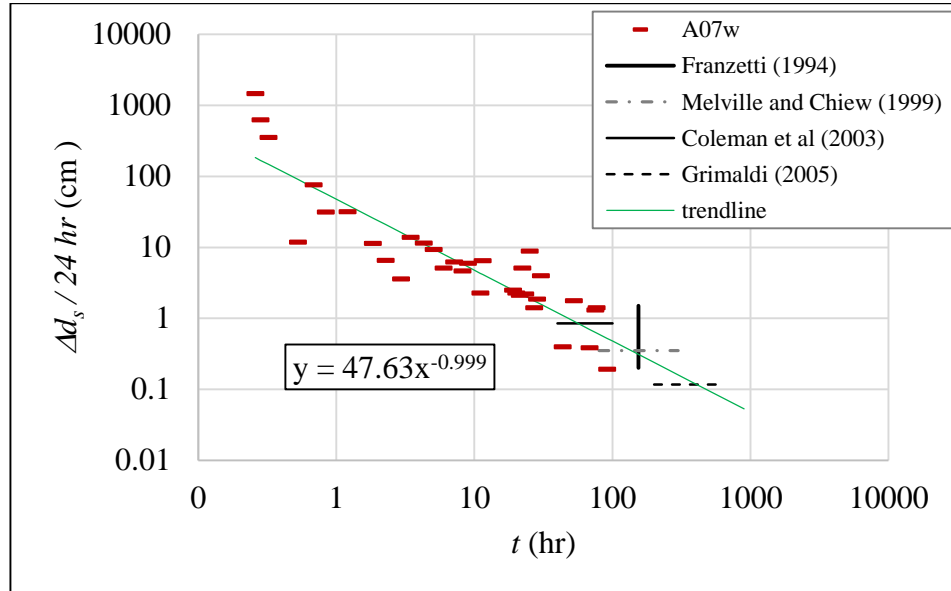THE TEMPORAL VARIATION OF SCOUR RATE $\varDelta d_s/24hr$ FOR ALL THE EXPERIMENTS

Figure A2.1 The variation of scour depth rate with respect to time for A07w.
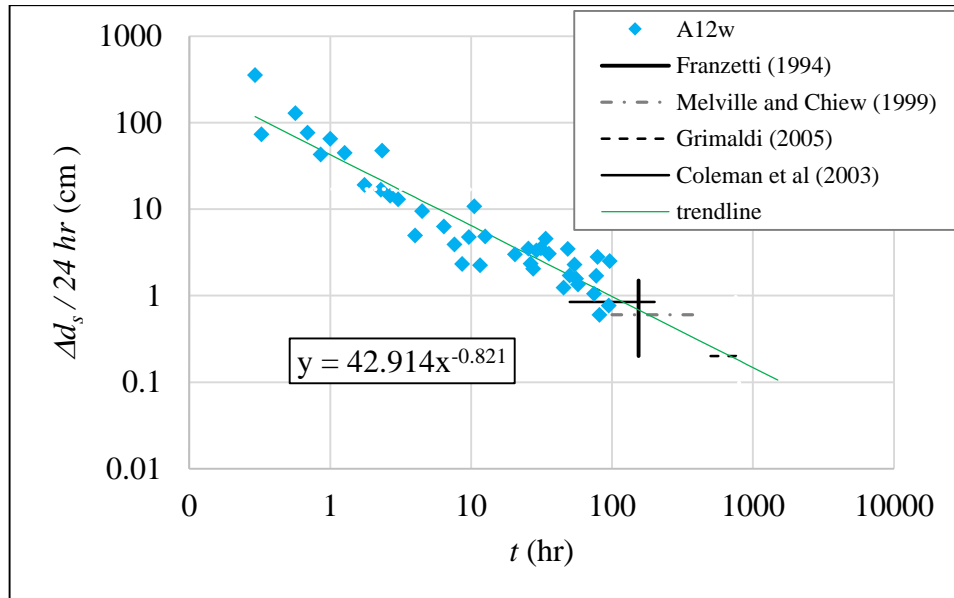

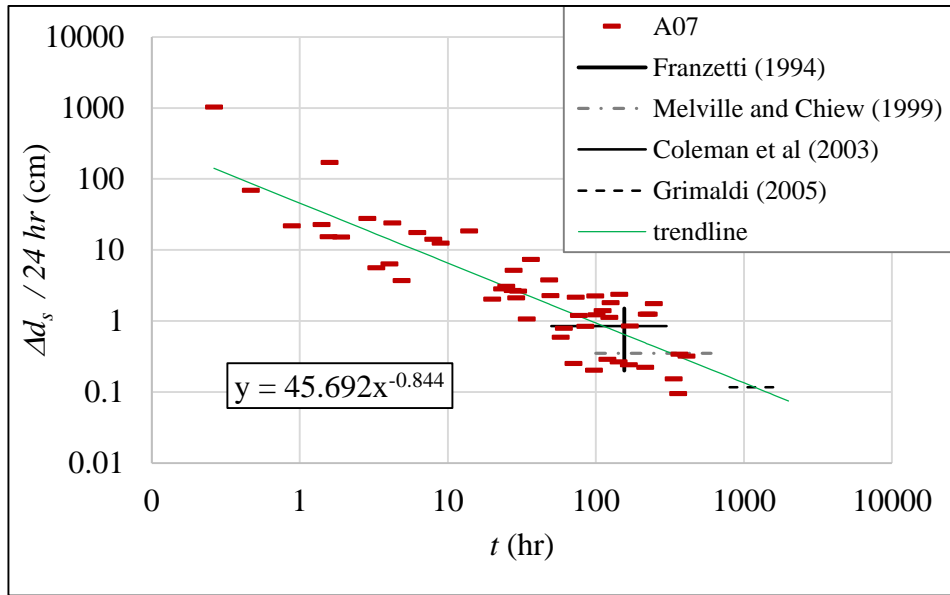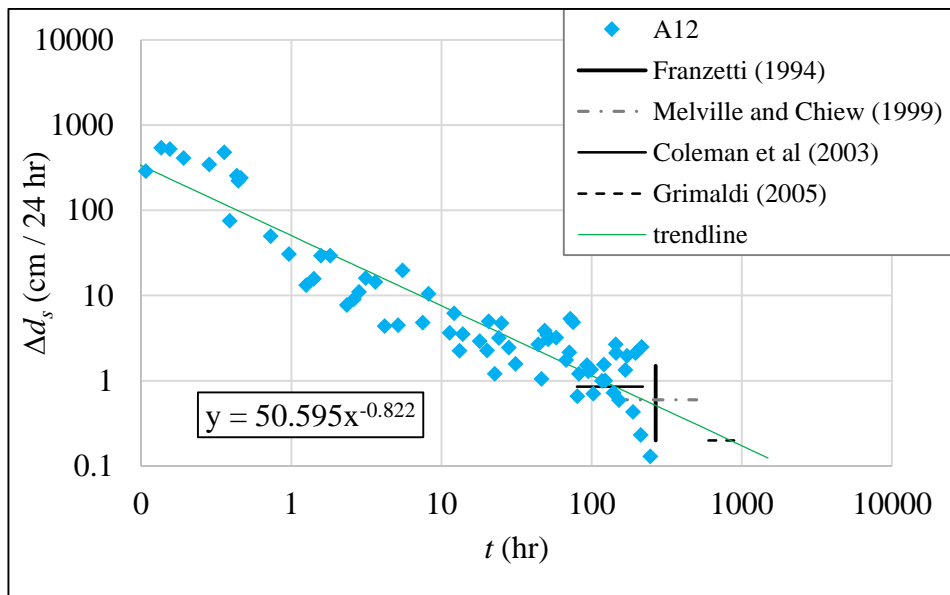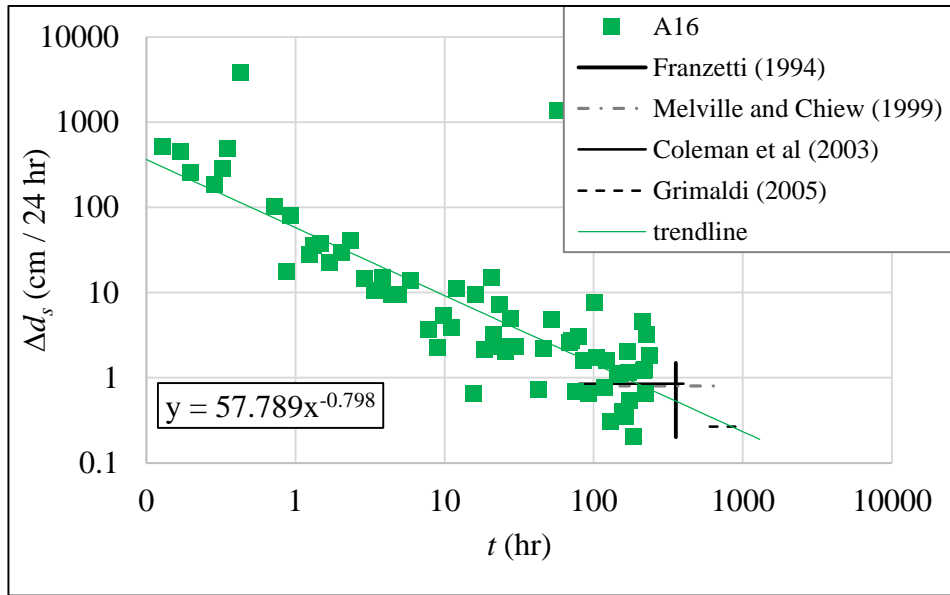**Figure A2.2** The variation of scour depth rate with respect to time for A12w.

Figure A2.3 The variation of scour depth rate with respect to time for A07.

Figure A2.4 The variation of scour depth rate with respect to time for A12.

Figure A2.5 The variation of scour depth rate with respect to time for A16.
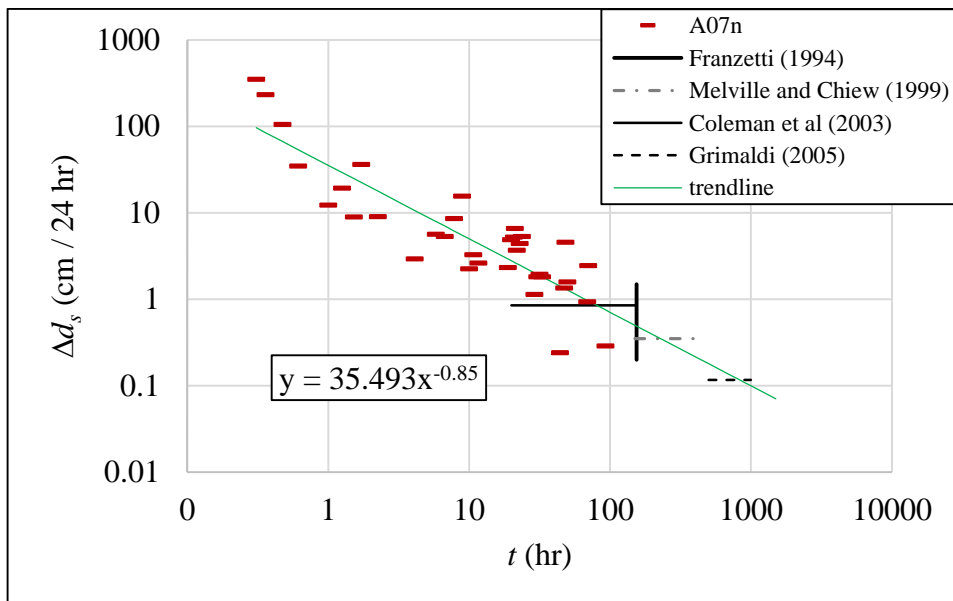

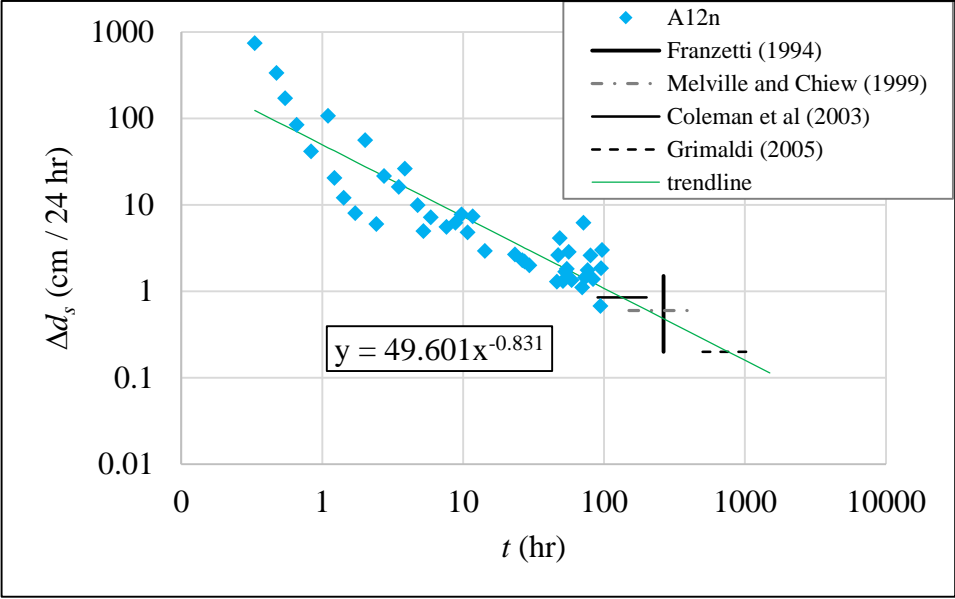**Figure A2.6** The variation of scour depth rate with respect to time for A07n.

Figure A2.7 The variation of scour depth rate with respect to time for A12n.

APPENDIX III

THE VARIATION OF DIMENSIONLESS SCOUR DEPTH WITH CONSTRICTION RATIO FOR FLOW SHALLOWNESS VALUES
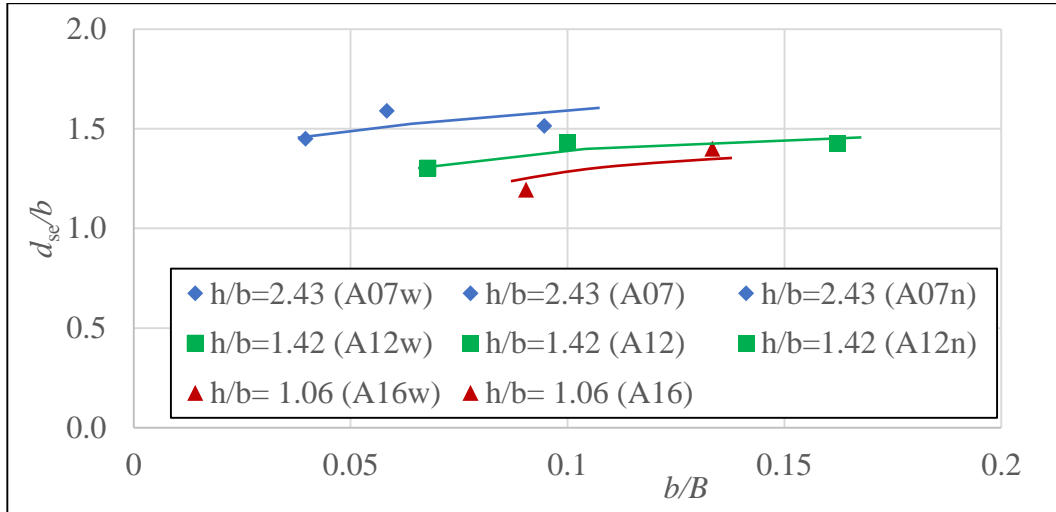

Figure A3.1 The equilibrium dimensionless scour depth with constriction ratio by (Franzetti et al. (1994)).
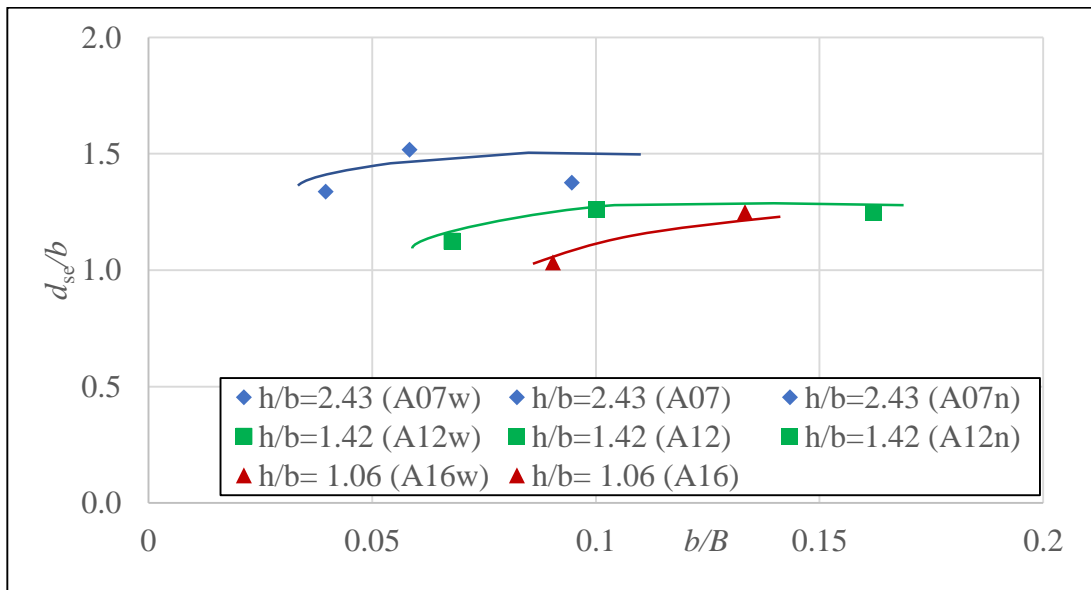

Figure A3.2 The equilibrium dimensionless scour depth with constriction ratio by (Coleman et al. (2003)).
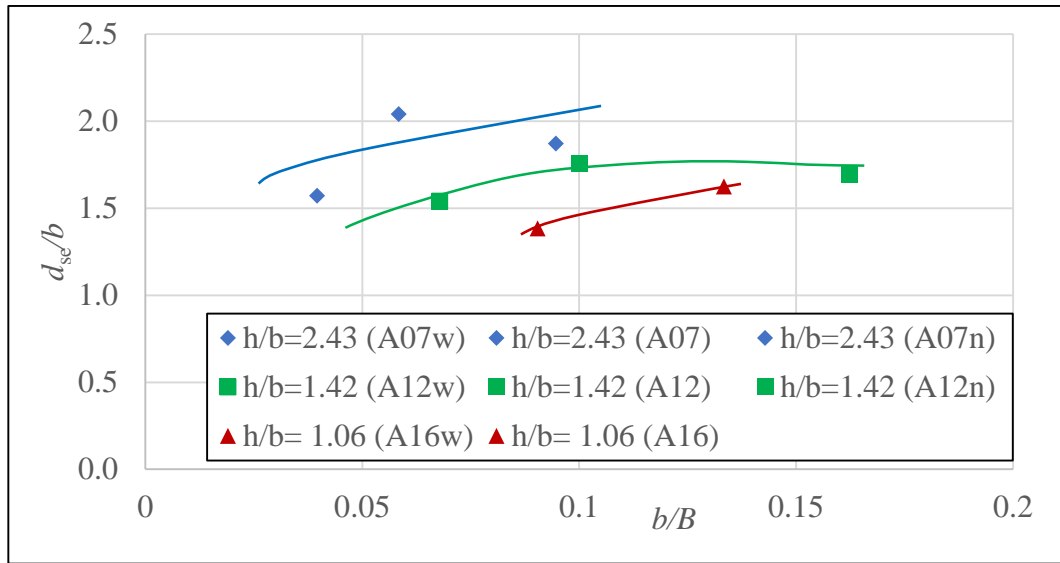
Figure A3.3 The equilibrium dimensionless scour depth with constriction ratio by (Grimaldi (2005)).

APPENDIX IV

SCATTER-PLOTS OF CALCULATED VERSUS OBSERVED DIMENSIONLESS
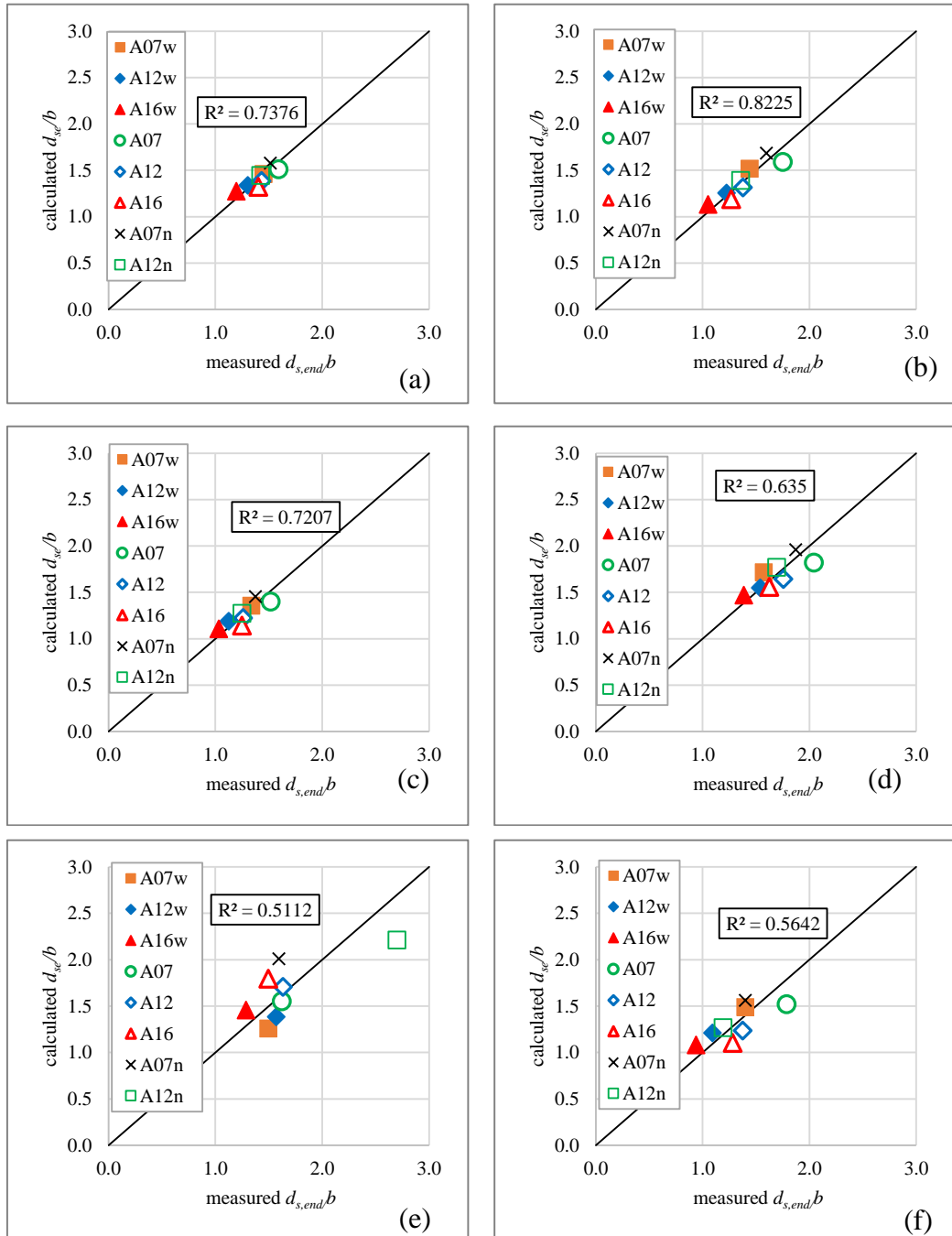SCOUR DEPTH

Figure A4.1 Scatter-plots of calculated versus observed dimensionless scour depth
(a) Franzettı et al. (1994), (b) Melville and Chiew (1999), (c) Coleman et al. (2003),
(d) Grimaldi (2005), (e) B_4, (f) Exp.

CURRICULUM VITAE

Name Surname: Waheedullah MOHAMMADKHAIL

Place and Date of Birth: Laghman / Afghanistan – 12/03/1994

Adress: İZMİR / TURKEY

E-Mail: sabawoon591@gmail.com, waheed.mohammadkhail@gmail.com

EDUCATION:

B.Sc.:

- İZMIR KATİP ÇELEBİ UNIVERSITY – FACULTY OF ENGINEERING AND ARCHITECTURE – CIVIL ENGINEERING DEPARTMENT (İZMIR / TURKEY) (2013-2018)

PUBLICATIONS:

- **Mohammadkhail, W.,** Bombar, G. (2019). "An Experimental Study on the Scour around Two in Line Circular Bridge Piers with Different Diameters". *3ᵗʰ International Student Science Congress, 3-4 May 2019 -* İzmir, Turkey.

ACCEPTED PUBLICATIONS:

- **Mohammadkhail, W.,** Bombar, G. (2020). "Scour problem around the bridge piers in Afghanistan". *4ᵗʰ. International Student Science Congress, 18-19 September 2020 -* İzmir, Turkey.

- **Mohammadkhail, W.,** Bombar, G., Eriş, E., İşler, Y., (2020). "Statistical Analysis of Monthly and Annual Precipitation and Monthly Mean Air Temperature in Black Sea (Turkey)". *4ᵗʰ. International Student Science Congress, 18-19 September 2020 -* İzmir, Turkey.

- **Mohammadkhail W.,** Bombar, G., Cardoso, A. H. (2020). "Effect of flow contraction on the bridge pier scour evolution". *14^{the} International conference on Hydroscience Engineering, September 2021* - İzmir, Turkey.

SCHOLARSHIP:

- Afghanistan Governmental Bachelor Degree Student Scholarship (September 2013 – July 2018)

- Master's Degree Student Scholarship. The Scientific and Technological Research Council of Turkey. Project No 116M519 (09 September 2018 – 01 March 2020)

COMPUTER SKILLS:

- AutoCAD

- Sap2000

- SPSS

- Ms Office

- GIS

- Matlab

- C++

CERTIFICATES:

- Certificate of Outstanding Achievement, İzmir Kâtip Çelebi University 2018

- Certificate of Participation, 3th International Student Science Congress (ISSC, 2019)

- Certificate of Appreciation, 3th International Student Science Congress (ISSC, 2019)

- Certificate of Participation, The International Student's Academy 2019

- Certificate of Participation, The International Student's Academy 2020

LANGUAGE SKILLS:

- Pashto (Native), English, Turkish and Persian